SYNTHESIS OF SOLID ACID CATALYST FROM RUBBER SEED SHELLS FOR BIODIESEL PRODUCTION

QUEK HUEI VERN

A project report submitted in partial fulfilment of the requirements for the award of Bachelor of Engineering (Hons.) Mechanical Engineering

Lee Kong Chian Faculty of Engineering and Science
Universiti Tunku Abdul Rahman

September 2017

DECLARATION

I hereby declare that this project report is based on my original work except for citations and quotations which have been duly acknowledged. I also declare that it has not been previously and concurrently submitted for any other degree or award at UTAR or other institutions.

Signature : _____

Name : _____

ID No. : _____

Date : _____

APPROVAL FOR SUBMISSION

I certify that this project report entitled **"SYNTHESIS OF SOLID ACID CATALYST FROM RUBBER SEED SHELLS FOR BIODIESEL PRODUCTION"** was prepared by **QUEK HUEI VERN** has met the required standard for submission in partial fulfilment of the requirements for the award of Bachelor of Engineering (Hons.) Chemical Engineering at Universiti Tunku Abdul Rahman.

Approved by,

Signature : _____

Supervisor : _____

Date : _____

Signature : _____

Co-Supervisor : _____

Date : _____

ACKNOWLEDGEMENTS

I would like to thank everyone who had contributed to the successful completion of this project. I would like to express my gratitude to my research supervisor, Dr. Steven Lim for his invaluable advice, guidance and his enormous patience throughout the development of the research.

In addition, I would also like to express my gratitude to my loving parents, who have been patient and understanding in giving me the time and space that I need to complete this research, and being there for me when I am at my lowest.

Moreover, I would like to thank my friends who not only gave me the help and encouragement I need to persevere throughout this project, but also lend a hand in brainstorming and making this research an enjoyable journey.

ABSTRACT

Sustainable energy has always been in the forefront of many green energy researches. The production of biodiesel using metal-based heterogeneous solid acid catalyst (SAC) comes with a great cost. In this study, a novel SAC using waste rubber seed shell was synthesised. A less conventional method of sulphonation using 4-benzenediazoniumsulphonate (4-BDS) was used to incorporate the active SO_3H group, resulting in the desired catalyst. Increasing the carbonisation temperature from 200 °C to 600 °C increased the porosity of the activated carbon, which further increased the specific surface area to a value of 238 m^2/g for SO_3H group attachments. Increasing the sulphanilic acid-to-activated carbon ratio from 2:1 to 10:1 during sulphonation increased the total acid density of the resulting catalyst until it reached the highest value of 2.894 $mmol/g_{cat}$. The free fatty acid (FFA) conversion of palm fatty acid distillate (PFAD) at 90 °C and 3 wt% catalyst loading was found to be dependent on the methanol-to-oil ratio (tested from 5:1 to 25:1) and the esterification duration (tested from 3 h to 8 h). Increasing the methanol-to-oil ratio to an optimum value of 15:1 and prolonging the duration up to 8 h enhanced the biodiesel conversion up to 30 %. This experiment justified the potential usage of waste rubber seed shells as a substitute for expensive metals in synthesising carbon-based catalysts for sustainable biodiesel production.

TABLE OF CONTENTS

LIST OF TABLES

LIST OF FIGURES

LIST OF SYMBOLS / ABBREVIATIONS

AV	acid value, mg KOH/g
AC	activated carbon
BET	Brunauer-Emmett-Teller
CCA	carbon-coated alumina
EA	elementary analysis
EDX	electron dispersive X-ray spectroscopy
FAME	fatty acid methyl esters
FFA	free fatty acid
FT-IR	Fourier Transform-Infrared Spectroscopy
HTC	hydrothermal carbonisation
MWCNT	multi-walled carbon nanotube
OPT	oil palm trunk
PAH	polycyclic aromatic hydrocarbons
PFAD	palm oil fatty distillate
POWC	palm oil waste cake
PTSA	p-toluenesulphonic acid
SAC	solid acid catalyst
SCB	sugarcane bagasse
SEM	scanning electron microscopy
TGA	thermogravimetric analysis
XRD	X-ray diffraction
XPS	X-ray photoelectron spectroscopy

LIST OF APPENDICES

CHAPTER 1

INTRODUCTION

1.1 Diesel and Biodiesel

Diesel fuel is a petroleum derivative produced from fractional distillation in the cracking process. Its higher volatility and carbon content in comparison with gasoline makes it an ideal transportation fuel for heavier vehicles like trucks and buses, construction equipment and military tanks (U.S. Energy Information Administration, 2016). Besides that, it is also used in diesel generators to generate electricity for small and medium-sized businesses (Diesel Service and Supply, 2017).

Biodiesel, on the other hand, is a non-fossil fuel alternative to its conventional counterpart, and is mostly produced from biomass such as vegetable oil and animal fats via esterification and transesterification. Like diesel, it is mainly utilised in diesel vehicles, whereby it is used in its pure form or as a biodiesel/diesel blend (Haluzan, 2010). Furthermore, biodiesel is used as fuel to heat up domestic and commercial boilers (Berkeleybiodiesel.org, 2015).

Table 1.1 below shows a comparison between diesel and biodiesel in terms of its properties, advantages and disadvantages.

Table 1.1: Comparison of Diesel and Biodiesel

Fuel	**Diesel**	**Biodiesel**	**References**
Source	Petroleum	Vegetable or animal oil	Haluzan, 2010
Lubrication	Poor	Significantly better	
Cetane number	Lower	Higher	
Flash point	64 °C (riskier)	130 °C (safer)	
Advantages	- Lower cost - Higher energy output	- Renewable, non-toxic, biodegradable - Fewer emissions of GHG - Low volatility - Better lubricity	Haluzan, 2010; Demshimino, et al, 2013
Disadvantages	- Non-renewable - Considerable amount of emissions (particulates, sulphur) - High volatility	- Nitrogen oxide emissions increase with fuel blending - Lower energy output - Higher cost	

1.2 Renewable Energy - Biofuel

The discovery and usage of renewable energy has been slow but on going over the years; it was not until the oil embargo set up by the Organisation of Petroleum Exporting Countries (OPEC) in the 1970s that made renewable energy a contingency plan to ensure continuous energy supply to the masses, and simultaneously reduce pollution (Ross, 2013). Global warming and the ozone layer depletion further solidified transnational efforts in saving the environment and promoting renewables, leading up to the formation of environmental organisations like Greenpeace International, European Renewable Energy Research Centers (EUREC) Agency, and the World Council on Renewable Energy (WCRE) (Martinot, 2008).

Biofuel consists of both bioethanol and biodiesel. Although it makes up the smallest percentage among the renewables (Figure 1.1), its continual contribution to the conservation of fossil fuels is welcomed. But crops have to be genetically engineered; land has to be cultivated for its growth; engines might need to be modified to run on biofuel (Biofuel.org.uk, 2017). Seeing as Earth's surface is roughly 71% seawater and 29 % land (Williams, 2016), it makes sense that some countries would rather use a more abundant and already-present source of energy compared to biodiesel, as can be interpreted from Figure 1.1. Furthermore, several countries are still experiencing famine, which resulted in the food insecurity issue.

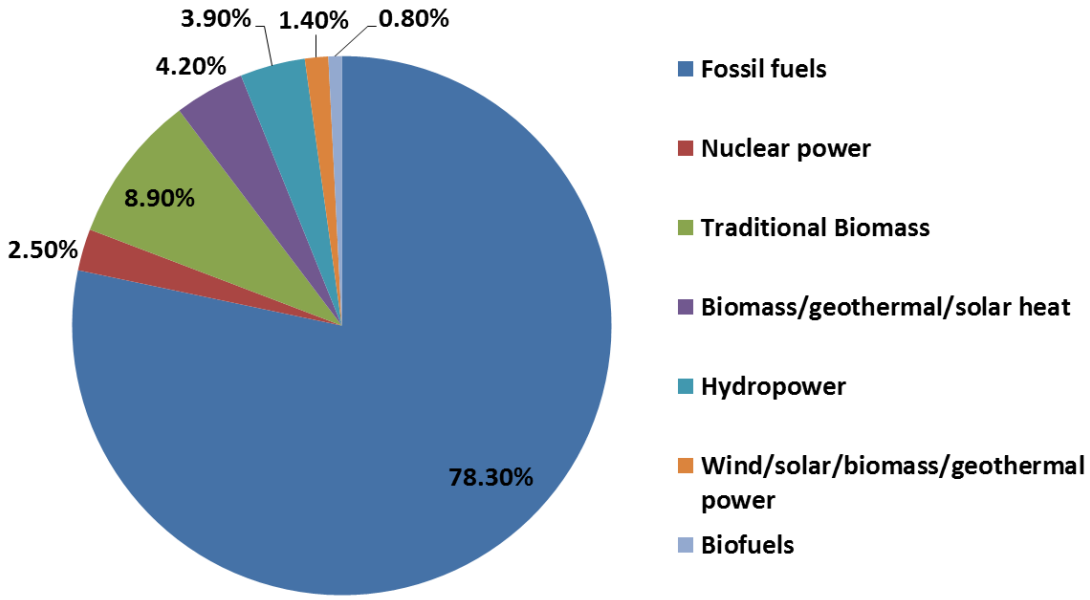

Figure 1.1: Estimated Renewable Energy Share of Global Final Energy Consumption in 2014 (REN21, 2016)

Within the 0.8% of biofuel produced, only 22% of it is biodiesel whereas bioethanol makes up 74%, with the remainder being hydrogenated vegetable oil. As most consumers drive gasoline-powered vehicles, there is a higher production of ethanol compared to biodiesel as like biodiesel, ethanol is blended with gasoline (U.S. Energy Information Administration, 2017). However, as the demand for both was maintained through blending mandates (B5, B7, B10, etc) the production of biofuel remains a competitive market.

1.2.1 Biodiesel Development Around the World

The consumption of biodiesel across the globe has been steadily increasing as the world begins the shift from using pure diesel fuel to diesel blends. Recently, Europe has remained as the largest biodiesel consumer, followed by the United States, Brazil, Asia, and the rest of the world (Merchant Research & Consulting, Ltd, 2017). The production of biodiesel continues to rise to keep up with global demands, with the United States in the lead, followed by Brazil, Germany, Argentina and France (REN21, 2016).

Overall, European Union is the world's largest biodiesel producer, representing about 80 % of the market. Its rapid production was motivated by growing crude oil prices, generous tax incentives (mostly in Germany and France), and the provisions on the production of oilseeds. Directives and mandates set out by the EU further encouraged biodiesel usage. Currently, France has a biodiesel mandate of 7.7% since 2014; Germany has a new mandate of 4.0 and Netherlands has an overall biofuel mandate of 7.75% (USDA Foreign Agricultural Service, 2016). Table 1.2 shows the main biodiesel producing members of the EU and their respective annual increment in production, with Germany leading with amounts ranging in the 3-billion liter range since 2010, followed by France, Netherlands, and Spain.

Table 1.2: EU Main Biodiesel Producers (Million Liters) (USDA Foreign Agricultural Service, 2016)

Calendar Year	2010	2011	2012	2013	2014	2015	2016	2017
Germany	3,181	3,408	3,106	3,307	3,808	3,351	3,350	3,410
France	2,295	2,090	2,516	2,476	2,681	2,442	2,215	2,390
Netherlands	434	558	1,337	1,562	1,954	1,988	1,990	1,990
Spain	1,041	787	545	668	1,016	1,103	1,070	1,080
Poland	432	414	673	736	786	795	800	800
Italy	908	704	326	521	658	665	665	665
Belgium	494	536	568	568	568	568	570	570
Portugal	328	419	356	307	325	440	443	455
Finland	375	253	320	399	409	409	440	440
United Kingdom	227	261	364	648	648	648	650	420
Others	992	1,611	971	791	488	1,126	1,487	1,935
Total	10,707	11,041	11,082	11,983	13,341	13,535	13,680	14,155

North and Latin America have also dominated the biodiesel trade. As a country by itself, the US remains to this day one of the major producers of biodiesel fuel, with Brazil not far behind. New targeted achievements continuously set up in the Renewable Fuel Standard (RFS) had helped the US produced about 4.8 billion litres of biodiesel, while Brazil had produced close to 4.1 billion litres in 2015 (REN21, 2016). B20 (20% biodiesel blended with 80% petroleum diesel) remains a common biodiesel blend in the US (U.S. Department of Energy, 2017). At the same time, in 2016, the Brazil biodiesel mandate had increased from B7 to B10 in 2019 (USDA Foreign Agricultural Service, 2016).

In Asia, biodiesel production fell drastically during 2015. Indonesia, who was once the top biodiesel producer in the world had 60% less production whereas China's biodiesel production has surged, which exceeded Indonesia's 2015 production levels. In February 2016, it was reported that China began putting more focus into its bioethanol production but had invested 1 billion euros in a biodiesel plant in Northern Finland (Kotrba, 2016). Indonesia had also started catching up, and achieved a production of 700 million litres in the first quarter of 2016 (USDA Foreign Agricultural Service, 2016).

1.2.2 Biodiesel Development in Malaysia

In Malaysia, under the National Biofuel Policy, which was released on March 21, 2006, the objectives were to use environmental-friendly and more sustainable energy sources to lower the fossil fuel dependency and to stabilise and lift palm oil prices.

Even though it was initially planned in 2008 to initiate the 5% biodiesel blend, it only began in 2011 and full nationwide implementation spanning both the peninsular region and East Malaysia was achieved in late 2014.

Growing crude palm oil stocks further pressured the Government to enact the B7 mandate in 2015. The 10% blending mandate, which was supposed to be implemented in July 2016, has since been postponed due to objections from industrial stakeholders – specifically concerns from vehicle suppliers about the apparent adverse impact of biofuel on diesel engine performance and lubrication systems, and also because the government has not achieved the B7 mandate (USDA Foreign Agricultural Service, 2016).

As shown in Figure 1.2, biodiesel production has been increasing unsteadily but is still far below full capacity as consumption still remains low. Furthermore, targeted biofuel values could not be met due to industry overcapacity and the Malaysian Government's freezing the supply of new licenses for biofuel processing plant. This has caused several of the plants to convert to oleo-chemical production, putting the expansion of biofuel blending plants to a halt (USDA Foreign Agricultural Service, 2016).

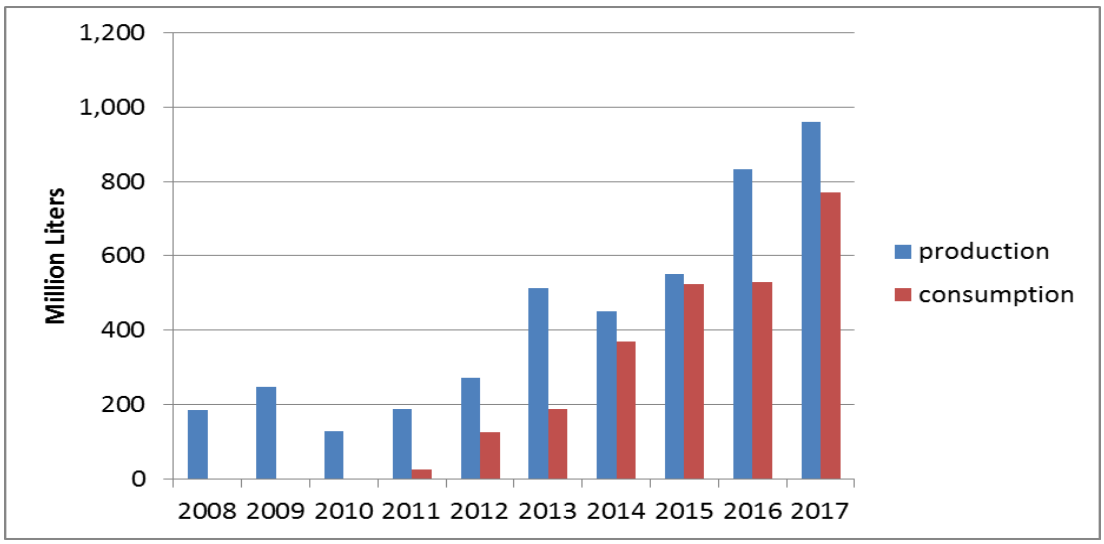

Figure 1.2: Malaysia Biodiesel Production and Consumption (USDA Foreign Agricultural Service, 2016)

1.3 Biodiesel Production

1.3.1 Biomass Waste as Feedstock

Food crops like maize, palm oil and soybeans are known to be utilised for the production of bioethanol and biodiesel. Besides obtaining these raw materials from edible crops, biofuel can also be derived from non-edible organic materials such as livestock manure, dead organisms, municipal waste and agricultural waste.

Agricultural waste normally found in crop residues can provide an alternative to fuel crops (crops planted for fuel), thereby reducing issues on proper land use and offer an alternative to crop burning by farmers through proper waste management. Table 1.3 shows the estimated crop residues produced in the United States and produced globally, and their corresponding oil equivalents. The estimates solidified the need of generating energy from crop residues such as wheat, soybeans, rapeseed, sugarcane, etc. to prevent the wastage of such energy potentials.

Table 1.3: Energy Value of Crop Residues Produced in the US and the World (Lal, 2005)

Parameter	USA	World
Total crop residue (10^6 Mg/year)	488	3758
Oil equivalent (10^6 barrels)	976	7560
Energy equivalent:		
Exajoules (10^{18} J)	9.1	69.9
Quads	8.0	60.0
10^{15} kcal	1.5	11.3

Malaysia has benefited much from the rubber industry ever since its introduction by the British colonists due to the country's ideal climate, soil and land (Hays, 2008). Its production has been increasing year by year as the usage of rubber became more versatile in making tyres for transport, consumer products such as gloves and hoses, and as adhesives and rubber vibration dampers in industry. Competition with neighbouring countries like Thailand and Vietnam had caused a decline in rubber prices between 1999 and 2004 but efforts were made to help local rubber manufacturers like Top Glove and Karex by providing a continuous supply of raw materials. Local authorities such as the Performance Management and Delivery

Unit (Pemandu) are distributing grants to smallholders to replant 40,000 hectares yearly and plant about 18,000 hectares worth of new areas over the next five years (Bloomberg News, 2012).

The sap cultivated from the rubber tree is often of importance, although the seed itself is used to extract its oil which can be used in the manufacture of paints, varnishes, inferior laundry soap, grease and biodiesel (Rubber Board, 2002). The shell produced from the removal of the kernel from the seed often finds its way to disposal sites or are burnt, although recent studies have started experimenting on its usage as a carbon precursor to activated carbon.

1.3.2 Esterification and Transesterification

Fatty acid methyl esters (FAME) are esters that can be treated as biodiesel through the esterification of fatty acids or the transesterification of triglycerides (Figure 1.3). Esterification is a reaction whereby an ester is formed when a carboxylic acid, such as a fatty acid, is mixed with an alcohol in the presence of acid catalyst. Transesterification, in contrast, involves the reaction of an ester or triglyceride (found in fats or oils) with an alcohol to form glycerol and the fatty acid alkyl esters – an acid or a base catalyst present, although base catalysts are more effective.

Both reactions are reversible and require the usage of a catalyst to speed up the rate of reaction. In order to shift the reactions' equilibriums forward to yield more biodiesel, a surplus of alcohol is needed to drive the reaction to the right hand side of the chemical equation to achieve a new equilibrium state, according to Le Chatelier's Principle (Clark, 2013).

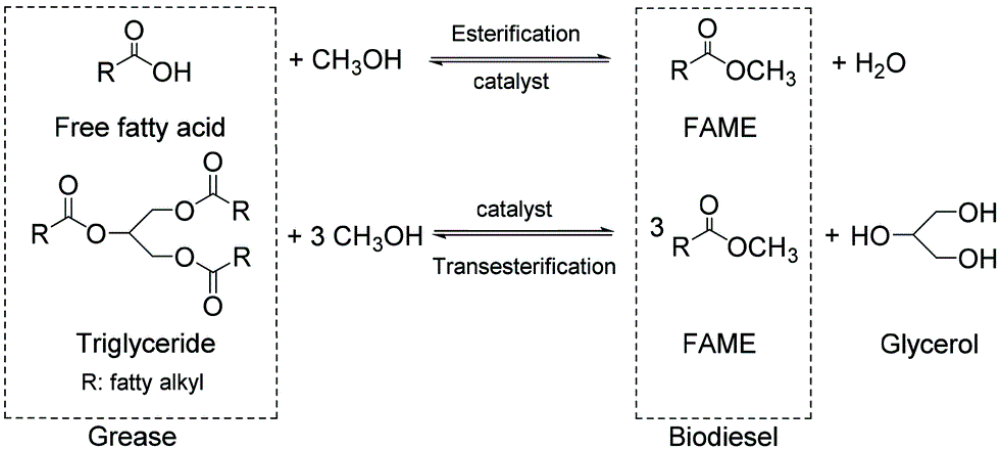

Figure 1.3: Transesterification of a Triglyceride and Esterification of a Fatty Acid Reaction (Zillillah, et al., 2014)

1.3.3 Types of Catalyst Used in the Industry

There are many types of catalyst involved in industrial processes as there is a need to obtain and supply goods on time. The main role of a catalyst is to increase the reaction rate (or shorten the time taken for a reaction) while it itself remains unconsumed. They can be classified into three main groups, but the former two are generally used in biodiesel production:

(i) Homogeneous catalyst – catalysts are in the same phase as the reactants.

(ii) Heterogeneous catalyst – catalysts are in a different phase compared to the reactants.

(iii) Enzymes – biological catalysts.

Furthermore, catalysts themselves can be derived from a variety of materials:

(i) Acids or bases (H_2SO_4 or NaOH).

(ii) Microorganisms (bacteria and yeast).

(iii) Biological molecules (enzymes like nitrile hydratase, glucose isomerase and galactosidase) (Choi, et al., 2015).

(iv) Transition metals (Vanadium(V) oxide, Titanium oxide).

1.4 Importance of the Study

By studying the effect of continual usage of crude oil derivatives on the environment and society, not only does this emphasize the severity of its impact in the ecology, it drives forward the need to switch from using non-renewable energy resources to a more continuous and sustainable supply of green energy.

Further reviews on the advancement of biodiesel production in various countries would provide a standpoint on one's current progress into the technology utilised in biodiesel production, encouraging the innovation and invention of newer, faster and more reliable production means. Not only that, by delving into the search for novel carbon-based solid acid catalysts, massive amounts of biomass wastes can be recycled and will not need to be disposed in landfills. This will lead to the discovery of a new niche in the production of renewable biofuels using a more sustainable method.

1.5 Problem Statement

The production of biodiesel has always been on-going, with increasing awareness on the need to practise sustainable development for the sake of the environment. Technology has constantly aid in the search for more cost-effective and safer production methods. These methods, which involve the usage of transition-metal supported catalysts; biocatalysts; acid-base catalysts, have their own advantages and disadvantages, and the pathway to finding a more plausible solution is never-ending.

Farmers worldwide, specifically in countries with a large agricultural sector, have been disposing their crop residues through open-burning, omitting the fact that the country is still facing severe environmental pollution. Also, biomass is abundant in municipal solid wastes, frequently ending up in landfills. The usage of biomass waste for the synthesis of a carbon-based solid acid catalyst for the production of biodiesel could kill two birds with one stone, encouraging renewable biofuel production, while gradually reducing landfill waste and encouraging an eco-friendlier way in disposing crop residues, especially in countries whereby their main source of income is through agricultural exports.

As Malaysia happens to be one of the world's largest rubber producers, it would come as no surprise if there were to be an abundance of rubber seed shells to be disposed from the removal of the rubber seed kernel for oil extraction. As little research has been done in using waste rubber seed shells to synthesis a carbon-based solid acid catalyst (SAC), this study hopes to utilise rubber seed shells in the synthesis of a novel SAC with low cost and optimum synthesis parameters.

1.6 Aims and Objectives

This study aims to find the optimum parameters to produce a heterogeneous catalyst derived from waste rubber seed shells to be used in catalysing the conversion of high FFA content waste to biodiesel.

There are several objectives to be achieved by the end of this research:

(i) To synthesise carbon-based solid acid catalyst using rubber seed shells through 4-benzenediazoniumsulphonate (4-BDS) sulphonation method.

(ii) To optimise the carbonisation temperature and sulphonation conditions (sulphanilic acid-to-activated carbon ratio) for the synthesis of the carbon-based solid acid catalyst.

(iii) To investigate the catalytic activity of the catalyst for biodiesel production by varying esterification conditions (methanol-to-oil ratio and esterification duration).

1.7 Scope of the Study

Chapter 1 would give a brief introduction as to the difference between diesel and biodiesel before delving into the oil depletion issue and the need for alternative fuel sources. Both global and local biodiesel production are briefly reviewed before introducing the use of catalyst in biodiesel production via the two main processes, esterification and transesterification.

Chapter 2 of this study would encompass various literature reviews that have been done regarding the production of solid acid catalysts from carbon-based sources, besides detailing the means of producing activated carbon before functionalising the material through the chosen sulphonation method.

Chapter 3 would then explain more on the methodology used in preparing and pretreating the rubber seed shells, carbonisation and functionalisation procedure of the raw material, before proceeding to its used as a catalyst in the production of biodiesel from palm oil fatty distillate.

Chapter 4 contains the results obtained from each parameter, which are the effect of carbonisation temperature on the specific surface area of activated carbon, the effect of sulphanilic acid-to-activated carbon ratio on the total acid density of the catalyst, the effect of methanol-to-oil ratio and the effect of esterification duration on the conversion of biodiesel.

Chapter 5 finally concludes the whole experiment and provides an overview as to the results obtained.

1.8 Contribution of the Study

This study aims to justify the finding that any type of carbon source can be used in synthesising a solid acid catalyst. As the purpose for this catalyst is to catalyse the esterification reaction, it would contribute to the biodiesel production industry as the waste generated from the manufacture of rubber-based product is in abundance. Furthermore, it can help identify the most suitable sulphonation method when it comes to functionalising a rubber seed shell-based catalyst.

CHAPTER 2

LITERATURE REVIEW

2.1 Comparison Between Different Types of Catalyst

As mentioned in Sub-subsection 1.1.3, there are three types of catalyst being employed in the biodiesel industry: homogeneous catalyst, heterogeneous catalyst, and biocatalyst. The choice in choosing which catalyst to used could depend on a number of factors. The ease at which it can be separated from the product, the costs and strength of the catalyst and the efficiency of both heat and mass transfer all play a role in determining the most efficient catalyst to apply.

The differences between each catalyst in terms of their advantages and disadvantages were compared in Table 2.1. It can be assumed from Table 2.1 that a suitable catalyst is an economical heterogeneous catalyst that has good heat and mass transfer, that can be separated easily, can be recycled and reused to save cost and insensitive to free fatty acid (FFA) content within the oil feed.

Table 2.1: Comparison of Homogeneous, Heterogeneous Catalyst and Biocatalyst (Talha and Sulaiman, 2016)

Type of catalyst	Derivative	Examples	Advantages	Disadvantages	References
Homogeneous catalyst	Base	NaOH, KOH, Alkali metal methoxides	- High selectivity in short duration - Low operating conditions - Good heat and mass transfer - Cheap and easily available	- Expensive separation costs - Sensitive to FFA content in oil - Lost of catalyst in saponification	CIEC Promoting Science, 2013; TutorVista.com, 2017; Talha and Sulaiman, 2016
	Acid	H_2SO_4, HCl, ferric sulphate	- Insensitive to FFA content in oil - Simultaneous esterification and transesterification - High biodiesel yield produced	- Can cause equipment corrosion - Costly separation - Low reaction rate	
Heterogeneous catalyst	Base	CaO, Vanadium(V) oxide, platinum, zeolite	- Simple separation - Catalyst can be recycled and reused - Long catalyst life time - Higher activity than its SAC - Moderate reaction conditions	- Low reaction rates - Sensitive to FFA content in oil - Problematic heat and mass transfer - Difficult to modify - Catalyst poisoning in ambient air	
	Acid	Tungsten oxides, sulphonated zirconia,	- Simple separation - Insensitive to FFA content in oil - Simultaneous esterification and transesterification - Can be regenerated and reused - Reduce corrosion problems	- Low reaction rates - Unfavourable side reaction - Higher cost - Leaching causes product contamination - High reaction conditions	
Enzyme		Algae, lipase	- Avoids soap formation - Simple recovery - Reusable and environmental friendly	- Very slow reaction rate - High cost - Deactivation at extreme conditions	Talha and Sulaiman, 2016

2.2 Carbon as a Source of Solid Acid Catalysts (SAC)

Inorganic heterogeneous acid catalysts such as tungstated zirconium oxide (Guldhe, et al., 2017), chromium-aluminium mixed oxide (Guldhe, et al., 2017), and $Ti(SO_4)O$ (Gardy, et al., 2016) had been used in recent studies for the production of biodiesel. However, several drawbacks are still present in their usage such as low acid site concentration, microporosity, hydrophilic character of catalyst surface, leaching of the active sites and high costs of synthesis (Shu, et al., 2009). On a good note, novel carbon-based solid acid catalysts are being developed with hopes of providing a more affordable alternative compared to their more expensive inorganic counterparts, despite having the same leaching and deactivation drawbacks.

Carbon is a chemical element widely found in most organic matter, be it edible or non-edible. It makes up the four main building blocks of life: carbohydrates, protein, lipids, and nucleic acid. Carbohydrate derivatives were observed to be good SAC catalysts as in the case of Lou, et al. (2008), whereby the catalysts were derived from carbohydrate powders of starch, cellulose, D-glucose and sucrose. Although the experiment indicated that the starch-derived catalyst achieved the highest yield in the shortest amount of time (83 % in 8 h compared with 80 % within 8 to 12 h), it still proved the feasibility of considering carbohydrates as a source of catalyst which still maintained high stability after 50 cycles of reuse.

Carbohydrate usage was further supported by Chen and Fang (2011), where a combination of carbohydrates was used, which is glucose and starch. The catalyst made from the glucose-corn starch mixture gave the highest fatty acid methyl ester (FAME) yield of 90 %. This finding was consistent with its structure that contained an acid site density of 6.373 mmol/g, which was the highest value among the other samples. Another recent synthesis was sulphonated-glucose acid catalysts derived from D-glucose catalyst made by Lokman, et al. (2015) and the resulting catalyst produced a biodiesel yield of 92.4 %.

Other polysaccharides like cellulose (Ayodele and Dawodu, 2014) and β-cyclodextrin (Fu, et al., 2015) were also produced as highly active and stable SACs. Ayodele and Dawodu (2014) had produced biodiesel from the esterification and transesterification of *Calophyllum inophyllum* oil using a cellulose-based catalyst, which produced a yield of almost 99 wt%. Its performance even surpassed that of the D-glucose derived catalyst that was used as a comparison. It managed to retain most

of its original transesterification activity, which was characteristic of carbon-based catalyst.

β-cyclodextrin was used as a precursor in the solid acid catalyst synthesis by Fu, et al. (2015). Compared with another well-known SAC, Amberlyst-15, it had a higher acid site density and larger pores for reactant accessibility to the active groups. Once again, the manufactured carbon-based catalyst maintained its stability up to six runs, although leaching of the active $–SO_3H$ group due to excessive alcohol washing slightly decreased the catalytic activity.

Non-edible waste biomass is also a rich source of carbon and many have begun the transition of using cheaper biomass waste. Shu, et al. (2009) had utilised vegetable oil asphalt to produce a carbon-based SAC catalyst, which gave a conversion of 89.93 % for cottonseed oil, an 80.5 wt% and 94.8 wt% conversion of triglycerides and FFA respectively in waste cooking oil (Shu, et al., 2010). In both experiments, the catalysts had high acid density, loose amorphous network and large pores, offering entry of reactants into the bulk where more acid sites were located. Furthermore, the acid sites were kept stable by the sulphonated polycyclic aromatic hydrocarbons (PAHs). Compared with other heterogeneous SACs, it could maintain its structure and acid sites at 270 °C, a high temperature characteristic of most acid-catalysed transesterifications. Also, it would not be deactivated in the presence of excess water produced from both reactions.

Novel catalysts were also synthesised from oil palm trunk (OPT) and sugarcane bagasse (SCB) by Ezebor, et al. (2014). The catalysts were successfully prepared, providing FAME yields of 88.8 % (OPT) and 96 % (SCB). The higher activity of SCB could be explained by its structure, which was flake-like compared to OPT, providing better attachment of the $–SO_3H$ groups during sulphonation. The study also showed the stability of both carbon-based catalysts as high catalytic activity still remained after 6 cycles, although the PAHs integrated with the $–SO_3H$ groups still leached out after each washing cycle.

Residual lignin contained in the hulls of *Xanthoceras sorbifolia* Bunge was used as a precursor in the development of a lignin-based solid acid catalyst by Guo, et al. (2012). Lignin is a non-carbohydrate biological polymer having cross-linked aromatic structures, making it a worthy candidate for the binding of the active $–SO_3H$ groups, which was further supported by FT-IR spectra analysis in the form of $C{-}O{-}SO_3H$. The FFA conversion achieved was as high as 97 %, and this value was

almost on par with the conversion achieved when using 1.5 wt% of sulphuric acid as a homogeneous catalyst. This study further highlights the significance of reusing biomass waste, especially those from the agricultural sector, as resourceful materials are still stored within. It is only a matter of discovery and finding a means of extracting the materials.

Besides conventional biomass waste as those listed above, another relatively cheap raw material, microalgae residue generated from its application in biodiesel production can be further processed to produce a novel SAC. Similar to producing a carbon-based SAC, Fu, et al. (2013) carbonized and sulphonated the microalgae residue, generating a catalyst comprising of aromatic carbon sheets (as cellulose was the main component of the microalgae) with high density of functional groups anchoring sites. The developed carbon SAC showed high catalytic activity, which persisted after 5 cycles with over 95 % conversion for esterification.

Table 2.2 provides an overview of the three inorganic SACs listed above and a comparison of their biodiesel production with SACs derived from both valuable and waste carbon sources. It can be seen that even cheap and unconventional raw materials could provide a biodiesel yield or conversion on par with those produced from costly metal-based catalysts.

In a nut shell, the abundance of carbon in life delivers a better alternative in synthesising carbon-based catalysts due to the high aromatic carbon content. Furthermore, efforts can be made in utilising waste biomass as a source of carbon as it would be more environmental friendly in terms of disposing waste in a more organised manner, relatively cheaper and ideal compared to exploiting useful and valuable metal and carbohydrate resources. Hence, rubber seed shells should be a viable candidate in the synthesis of a biomass-based SAC in the production of biodiesel, further expanding its usage as an activated carbon. In addition, it could reduce waste residual and incite proper waste disposal methods after obtaining the kernel from the rubber seed.

Not only that, the literature review from various sources in Table 2.2 depicted that an ideal heterogeneous carbon-based solid acid catalyst should have diverse pore structure, high catalytic stability, high catalytic activity, high acid site density, hydrophobicity that prevents catalyst deactivation by water generated from esterification, hydrophilic functional groups that provide methanol access to the triglyceride and FFA molecules, and low cost.

Table 2.2: Inorganic and Organic Catalyst Used in Biodiesel Production

Catalyst Derivation	Catalyst Characterisation	Feedstock	Esterification & Transesterification conditions				Yield(Y) or Conversion (C) (%)	Reference
			Alcohol to oil molar ratio	Time (h)	Temperature (°C)	Catalyst loading (wt%)		
Ti(SO4)O	Average particle size: 45 nm BET surface area: 44.4563 m^2/g Average pore size: 22 nm	Used cooking oil	9:1	3	75	1.5	97.1 % (Y)	Gardy, et al. (2016)
Tungstated zirconia	N/A	Microalgae lipids	12:1	3	100	15	94.58 % (C)	Guldhe, et al. (2016)
Cr-Al catalyst	BET surface area: 56 m^2/g Acidity: 182.28 µmol/g Pore size: 2.9-7.0 µm	Microalgae lipids	20:1	3	80	15	97.75 % (C)	Guldhe, et al. (2016)
Starch from Carbohydrate powder	Average pore volume: 0.81 cm^2/g Average pore size: 8.2 nm BET surface area: 7.2 m^2/g Acid site density: 1.83 mmol/g	Waste cooking oil	30:1	8	80	10	92 % (Y)	Lou, et al. (2008)
Glucose-corn powder mixture	Acid site density: 6.373 mmol/g	Waste cottonseed oil	10:1	6	80	5	96 % (Y)	Chen and Fang (2011)
D-glucose	BET surface area: 10.67 m^2/g Acid site density: 1.88 mmol/g	Palm fatty acid distillate	12.2:1	134 min	65	2.9	92.4 % (Y)	Lokman, et al. (2015)

Table 2.2: (continued)

Catalyst Derivation	Catalyst Characterisation	Feedstock	Esterification & Transesterification conditions				Yield(Y) or Conversion (C) (%)	Reference
			Alcohol to oil molar ratio	Time (h)	Temperature (°C)	Catalyst loading (wt%)		
Cellulose	Surface area: 2.4 m^2/g Total acid density: 3.9 mmol/g	*Calophyllum inophyllum* oil	15:1	4	180	5	~99 % (Y)	Ayodele and Dawodu (2014)
B-cyclodextrin	BET surface area: 5.6 m^2/g Sulphur concentration: 0.86 mmol/g	Mixed oil of oleic acid and triolein	30:1	12	85	5	~80 % (Y)	Fu, et al. (2015)
Vegetable oil asphalt	Average pore diameter: 43.9 nm BET surface area: 7.48 m^2/g Acid site density: 2.21 mmol/g	Refined cottonseed oil	18.2:1	2.5	260	1	89.93 % (C)	Shu, et al. (2009)
		Waste cooking oil	16.8:1	4.5	220	0.2	94.8 % FFA (C) 80.5 % triglyceride (C)	Shu, et al. (2010)
Oil palm trunk	Acid site density: 0.81	Palmitic acid	18:1	5	65	9	88.8 % (Y)	Ezebor. et al. (2014)
Sugarcane bagasse	Acid site density: 1.41						96 % (Y)	
Lignin-derived from husk	BET surface area: 4.7 m^2/g Acid site density: 0.86 mmol/g	Acidified soybean soapstock	9:1	5	70	7	97 % (C)	Guo, et al. (2012)
Microalgae residue	BET surface area: > 1 m^2/g Acid site density: 0.90 mmol/g	Oleic acid and triglyceride	N/A	12	80	5	98 % FFA (C) 24 % triglyceride (Y)	Fu, et al. (2013)

2.3 Carbonisation of Biomass

As carbon-based catalysts are becoming the norm in the production of biofuel, there is a need to synthesis said catalyst which offers high catalytic activity, stability, diverse pore structure and high acid density sites. Generally, carbon can be classified into two variants, namely crystalline carbons and amorphous carbons. It has been discovered that amorphous carbons such as the traditional activated carbons and biochars, offers scientists the more promising surface structure due to its high micropore and mesopore volumes coupled with the resulting high surface area, increasing the sites for the active group attachments (Yang, et al., 2011).

2.3.1 Synthesis of a Porous Carbonaceous Structure

De, et al. (2015) had described in their literature the common ways of producing porous carbon from biomass precursors based on three methods: hydrothermal carbonisation (HTC), template-directed synthesis, and direct synthesis method. Hydrothermal carbonisation is considered the most widely applied and favourable approach and can be further subdivided into two types: high-temperature HTC and low-temperature HTC:

(i) High-temperature carbonisation process is carried out under supercritical water. It can penetrate into the pore structure better to produce a broader distribution of micro- and mesopores and is highly useful in preparing dissimilar carbon-based materials with high surface areas and porosity. The disadvantage of this method is the high operating temperature (300 – 800 °C) could clearly bring about an adverse effect to when it comes to the stability of standard organic compounds.

(ii) Low-temperature carbonisation process is a more benign approach performed up to 250 °C and can be used for the functionalization of activated carbon by dehydration, condensation, polymerisation and aromatisation reactions; but its procedure is quite complex as it involves the generation of different soluble products.

Another carbonisation method is the template-directed synthesis method, and as its name depicts, applies the usage of a template for the creation of carbonaceous materials with well-ordered pore size distribution. Three templates can be utilised,

that is hard template, soft template and dual template. Regardless of the type of template used, it only serves as a scaffold, directing the pore formations during the carbonisation process and hence improving the level of structural ordering (De, et al., 2015). Its downside is that the structure obtained after its removal from the template collapses at extreme temperatures.

Direct synthesis carbonisation leads to the formation of Starbons – a novel class of mesoporous carbonaceous materials with adjustable surface functionalities. This method is not only simple and environmental friendly as the HTC method; it is applicable to the carbonisation of non-porous raw materials with low surface areas. Besides that, there is no need for a template and it can be performed within various temperature ranges (eg. 200 – 1000 °C), producing a structure with outstanding pore volumes and sizes (De, et al., 2015). Table 2.2 illustrates several examples of the direct synthesis carbonisation methods used in numerous literatures.

Table 2.3: Different Carbonisation Methods from Various Literatures

Carbon source	**Carbonisation method**	**Sulphonation method**	**Reference**
Corn straw	2 g of material were heated under N_2 flow for 1 h at different temperatures (250, 300, 350, 400, 450, 500 °C)	Direct sulphonation with fuming H_2SO_4	Liu, et al. (2013)
Microcrystalline Cellulose	50 g of material was pyrolysed under dry N_2 at 400 °C for 5 h	Direct sulphonation with conc. H_2SO_4	Ayodele and Dawodu (2014)
D-glucose	15 g of material were heated at 400 °C for 12 h in an inert environment	Direct sulphonation with conc. H_2SO_4	Lokman, et al. (2015)
Sucrose-Al_2O_3 composite	Composite was carbonised at 600 °C under N_2 gas.	Sulphonation by 4-BDS	Geng, et al. (2011)
Oil-cake waste	20 g of powdered material was impregnated with 50 % ortho-phosphoric acid for 24 h before being calcined in a muffle furnace at 500 °C for 1 h. Material was then washed with double distilled water, HCl and hot double distilled water to obtain a pH of 6-7 before drying in an oven at 110 °C.	Sulphonation by 4-BDS	Konwar, et al. (2014)

2.3.2 Carbonisation Temperature and Time on Catalytic Performance

Lou, et al. (2008) found that the temperature and time of carbonisation had a significant effect on the catalytic performance. Based on the study, increasing the carbonisation temperature of a starch-based catalyst from 300 °C up to 400 °C showed an increase in catalytic activity and biodiesel yield of 24.8 %. Any further increment caused a noticeable decline in performance. It was deduced that at low temperatures, water produced from the reaction can be adsorbed onto the catalyst exterior to prevent the entry of relatively hydrophobic oil samples, and cause the leaching of the active groups due to the formation of a soft aggregate with weaker bonding; high temperatures caused the catalyst to be rigid, and contained fewer –

SO_3H groups. Besides, the study showed that prolonging carbonisation time could increase yield until it reached a peak at 15 h of carbonisation before declining.

The study done by Lou, et al. (2012) showed once again that carbonisation temperature contributed a lot to the development of a novel solid acid catalyst as the bagasse-derived catalyst became more active as temperature of carbonisation increased. Their results were attributed to the findings whereby increasing the carbonisation temperature produced a rigid yet flexible structure with polycyclic aromatic sheets (Lou, et al., 2008). The results obtained in the 2012 study are summarised in Figure 2.1, which illustrated the minute dependence of carbonisation time and greater dependence of carbonisation temperature for the resulting bagasse-derived catalyst.

Geng, et al. (2012) also confirmed the effect of carbonisation temperature on the performance of the final catalyst. The results showed that at high carbonisation temperatures (up to 1000 °C), the carbon content within the sample increased, increasing the number of sites for SO_3H attachment. Although, the number of oxygen-containing active sites (which did not play a major role in esterification and transesterification) reduced. Furthermore, the higher the carbonisation temperature, the greater the BET surface area obtained, which was beneficial to prevent the porous carbonaceous structure from collapsing with the formation of a more rigid structure.

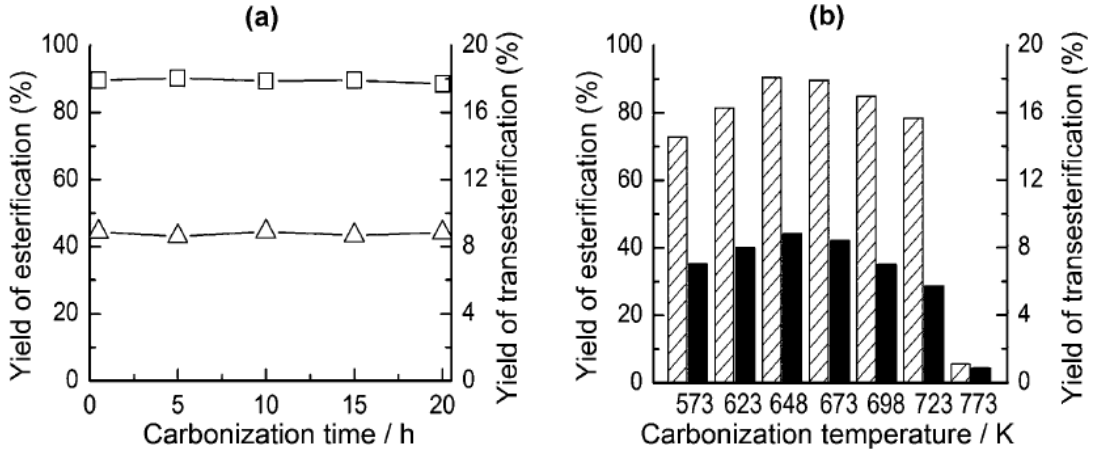

Figure 2.1: Influence of (a) Carbonisation Time; and (b) Carbonisation Temperature on Esterification (□ and striped bars) and Transesterification (△ and black bars) Activities of Bagasse-Derived Catalysts (Lou, et al., 2012)

The study done by Liu, et al. (2013) also showed that catalytic activity changes with changing carbonisation temperatures. As can be seen in Figure 2.2, at constant carbonisation duration, the ester yield obtained by the esterification of oleic acid with corn-straw-based catalyst varied with temperature. It could be inferred that at carbonisation time of more than 1 h, the optimum carbonisation temperature would be within 550 to 600 K (277 – 327 °C).

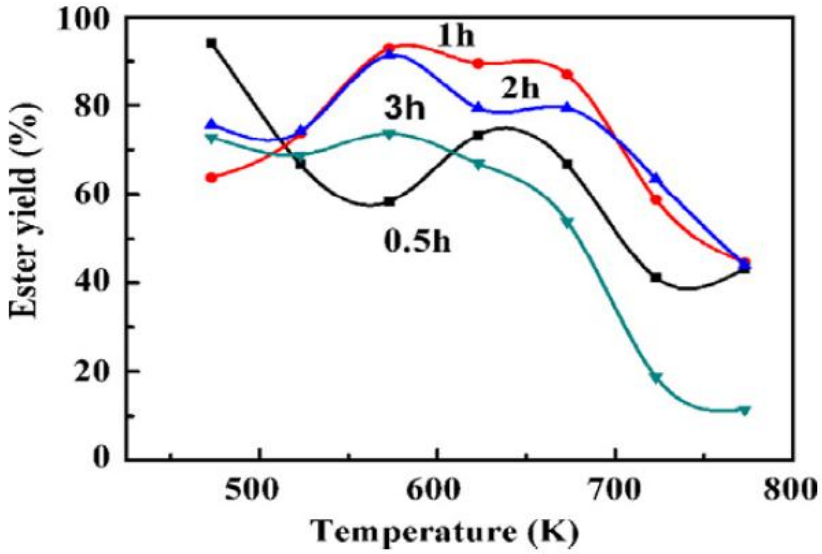

Figure 2.2: Influence of Carbonization Time and Carbonization Temperature on the Ester Yield (Liu, et al., 2013)

As mentioned previously, Lou, et al. (2008) had studied the effect of carbonisation time on the methyl oleate yield and concluded that prolonging carbonisation time could increase yield until it reached a peak at 15 h of carbonisation before declining. Mo, et al. (2008) also investigated the effect of carbonisation duration on catalytic performance and the study showed that increasing carbonisation duration up to 5 h started reducing the acetic acid conversion by 2.1 % for the D-glucose-derived catalyst. When the carbonisation time was prolonged up to 15 h, there was a 3 % decrease in conversion.

Both studies clearly showed the effect that carbonisation time had on catalytic performance, but the immediate decrease in performance of the catalyst derived by Mo, et al. could be attributed to the higher carbonisation temperature (400 °C) as compared to that of Lou, et al. (150 °C). Later in 2012, Lou, et al. conducted their experiment on sugarcane bagasse and the results showed that carbonisation duration

had no significant effect on the yield of esterification and transesterification, as prolonging carbonisation time only resulted in imperceptible fluctuations in yield, as illustrated in Figure 2.1 (a), which was consistent with the findings made by Mo, et al. (2008).

The study carried out by Dawodu, et al. (2014) further supported the findings made by Mo, et al. (2008) regarding the effect of carbonisation time on catalytic performance. According to the acid density results obtained, the catalyst prepared from materials carbonised for 1 h had a greater amount of smaller carbon sheets and consequently higher $–SO_3H$ densities (especially those attached to the sheet edges) than the catalyst synthesised from substances carbonised for 5 h (Dawodu, et al., 2014), although no findings were done on why was it so.

Therefore, it can be concluded that regardless of the type of starting materials used to synthesise carbon-based solid acid catalysts, carbonisation temperature plays a more significant role than carbonisation time.

2.4 Sulphonation

Once carbonisation has taken place in producing the activated carbons, there is a need to increase the density of the acid sites on the carbonaceous surfaces as the existing acid sites – OH and COOH groups – only result in mild FFA conversion during esterification and transesterification. Hence, like normal esterification methods, an activating agent is needed to provide a means of bringing both reactant molecules, which in this case are the FFA or triglyceride molecules and alcohol, close enough to establish a temporary bond and react.

2.4.1 Sulphonation methods

According to De, et al. (2015), there were numerous ways to functionalise carbonaceous materials:

(i) Direct/in situ functionalization – organic or inorganic materials containing the functional groups were mixed directly with the catalytic material during its synthesis.

(ii) Post-synthetic modification – the functional groups were inserted after the carbonaceous supports were prepared.

The second approach is more widely applied as compared to the single-step direct functionalization process as certain modifications cannot be done at the temperature of carbonisation (De, et al., 2015). Functionalisation can be done via sulphonation or carbon nanocomposites, but sulphonisation would be utilised in this report.

Sulphonated carbon can be prepared by directly pyrolysing and sulphonating the carbon precursor in concentrated sulphuric acid (H_2SO_4). Although simple, this process usually produces a catalyst with low surface area, low acid site densities and poor diffusion in liquid-phase reaction mixtures (Geng, et al., 2011). Lou, et al. (2008) had reported that higher catalytic activity was observed with larger BET surface area, pore volume and pore size, especially if the $-SO_3H$ groups were also found in the catalyst bulk. In their experiment, the comparatively larger pore size and pore volume of the starch-based catalyst enabled the reactants to enter and reach the active sites within the bulk, leading to higher catalytic efficiency compared to those of cellulose, sucrose and D-glucose (Lou, et al., 2008). Hence, it is more favourable to obtain a carbon catalyst with high porosity and surface area coupled with high acid densities.

In addition, sulphonation using strong sulphonating agents like concentrated sulphuric acid or fuming sulphuric acid were carried out at high temperatures (150 – 250 °C); the process was not entirely friendly (Konwar, et al., 2015). Furthermore, sulphuric acid was reportedly incapable for sulphonating aromatised, structured and rigid carbon materials (graphite, activated carbons or carbonised carbon material). Thus, it is highly difficult to produce a catalyst which has both high porosity (as sulphonation reduces porosity) and acid density via direct sulphonation of concentrated or fuming sulphuric acid (Konwar, et al., 2015).

On the other hand, functionalised sulphonation using 4-benzenediazoniumsulphonate (4-BDS) radicals will be more preferable instead of H_2SO_4 as it utilises milder conditions (around 5 °C), preserves the structural and morphological properties of the support, and it has the ability to sulphonate more rigid and aligned carbon structures (activated carbon, graphene, ordered mesoporous carbons, etc). Hence, it can be surmised that sulphonation via the 4-BDS method provided a higher acid density, even higher than the acid density obtained through sulphonation with H_2SO_4 making it appropriate for the functionalization of carbon materials with thin walls, large pores, and large BET surface areas (De, et al., 2015).

Sulphonation can also be done via *p*-toluenesulphonic acid (PTSA) as was done by Dawodu, et al. (2014). Although, materials sulphonated with concentrated H_2SO_4 had a higher sulphur content than PTSA, which indicated a higher acid density. Besides sulphonating multi-walled carbon nanotubes (MWCNTs) with concentrated H_2SO_4, Shuit and Tan (2014) had also sulphonated the nanotubes via other means as thermal treatment with H_2SO_4 was time-consuming and energy-intensive. The study showed that among concentrated H_2SO_4, in-situ polymerisation of acetic anhydride and sulphuric acid, in-situ polymerisation of poly(sodium 4-styrenesulphonate) and the thermal decomposition of ammonium sulphate, the usage of poly(sodium 4-styrenesulphonate) synthesised a catalyst with the highest acid site density, achieving the highest yield of 93.4 % amongst the four. Table 2.4 provides a general outlook on the methods of sulphonation from various literatures.

Table 2.4: Sulphonation Methods Utilised by Various Literatures

Sulphonation method	Carbon source	Catalyst Characterisation	Esterification & Transesterification conditions			Reference
			Operating conditions	Yield(Y)/ Conversion (C)/ Turnover frequency (TOF)	Recyclability	
Direct sulphonation with fuming H_2SO_4	Micro-crystalline cellulose powder	Particle size = 10 – 40 µm BET surface area = 2 m^2/g Acid site density = 1.9 mmol/g	Esterification: Feedstock = Oleic acid Alcohol:oil ratio = 25.8:1 Time = 4 hours Temperature = 368 K Loading = 4.6 wt%	Y = 99.9 %	Washed with water: no decrease in yield even after 10 cycles Washed with methanol: activity decrease to 75-80% yield after 4 cycles	Hara (2010)
			Transesterification: Feedstock = trolein Alcohol:oil ratio = 62:1 Time = 5 hours Temperature = 403 K Loading = 6.77 wt%	Y = 98.1 %	Washed with water: activity remains high even after 5 cycles	
Direct sulphonation with fuming H_2SO_4	Oil palm trunk	Acid site density = 1.41 mmol/g Total acid site density = 5.31 mmol/g	Feedstock = Palmitic acid Alcohol:oil ratio = 18:1 Time = 5 hours Temperature = 65 °C Loading = 9 wt%	Y = 88.8 %	Washed with n-hexane: yield decreased to 79.5% after 6 cycles	Ezerbor, et al. (2014)
	Sugarcane bagasse	Acid site density = 1.53 mmol/g Total acid site density = 5.52 mmol/g		Y = 96 %	Washed with n-hexane: yield decreased to 84% after 6 cycles	
Direct sulphonation with concentrated H_2SO_4	Sugarcane bagasse	Acid site density = 1.06 mmol/g Total acid site density = 3.69 mmol/g	Feedstock = Oleic acid Alcohol:oil ratio = 10:1 Time = 6 hours Temperature = 80 °C Loading = 0.14 g	Y = 95 %	Washed with n-hexane: activity still remains around 90% after 8 cycles	Lou, et al. (2012)

Table 2.4: (continued)

Sulphonation method	Carbon source	Catalyst Characterisation	Esterification & Transesterification conditions			Reference
			Operating conditions	Yield(Y)/ Conversion (C)/ Turnover frequency (TOF)	Recyclability	
Sulphonation with 4-BDS	Activated carbon powder	BET area = 318 m^2/g Average pore diameter = 2.36 nm Pore volume = 0.76 cm^3/g Acid density = 1.42 mmol/g	Feedstock = Oleic acid Alcohol:oil = 8 mL:1g Time = 6 hours Temperature = 65 °C Loading = 50 mg	TOF = 44 h^{-1}	-	Geng, et al. (2011)
	Carbon-coated alumina (CCA)	BET area = 39 m^2/g Average pore diameter = n.d. Pore volume = 0.04 cm^3/g Acid density = 1.72 mmol/g	Feedstock = Oleic acid Alcohol:oil = 8 mL:1g Time = 6 hours Temperature = 65 °C Loading = 50 mg	TOF = 78 h^{-1} (almost five times of Amberlyst-15 (15 h^{-1}))	-	
	Carbon-coated alumina (CCA) with alumina removed	BET area = 354 m^2/g Average pore diameter = 2.83 nm Pore volume = 0.25 cm^3/g Acid density = 1.49 mmol/g	Feedstock = Oleic acid Alcohol:oil = 8 mL:1g Time = 6 hours Temperature = 65 °C Loading = 50 mg	TOF = 109 h^{-1} (almost five times of Amberlyst-15 (15 h^{-1}))	-	
Sulphonation with 4-BDS	Oil-cake waste (OCW)	Acid density = 0.735 mmol/g Total acid density = 2.426 mmol/g BET area = 556 m^2/g Average pore diameter = 3.9 nm Micropore volume = 0.20 cm^3/g	Feedstock = Jatropha oil Alcohol:oil 43:1 Time = 6 hours Temperature = 80 °C Loading = 3 wt%	C = 99 %	Conversion remains above 90% after 5 cycles	Konwar, et al. (2014)

Table 2.4: (continued)

Sulphonation method	Carbon source	Catalyst Characterisation	Esterification & Transesterification conditions			Reference
			Operating conditions	Yield(Y)/ Conversion (C)/ Turnover frequency (TOF)	Recyclability	
Sulphonation with 4-BDS	*J.curcas* De-oiled seed waste cake (DOWC)	Acid density = 0.70 mmol/g Total acid density = 3.96 mmol/g BET area = 93 m^2/g Average pore diameter = 3.9 nm Total pore volume = 0.23 cm^3/g	Feedstock = Oleic acid Alcohol:oil 20:1 Time = 10 hours Temperature = 64 °C Loading = 3 wt%	TOF = 70.81 h^{-1}	Maintain high conversion at above 60 % after 3 cycles	Konwar, et al. (2015)
	P. pinnata De-oiled seed waste cake (DOWC)	Acid density = 0.84 mmol/g Total acid density = 3.62 mmol/g BET area = 483 m^2/g Average pore diameter = 4.8 nm Total pore volume = 0.46 cm^3/g		TOF = 104 h^{-1}	Maintain high conversion at above 60 % after 3 cycles	
Sulphonation with 4-BDS	*M. ferrea* L. De-oiled seed waste cake (DOWC)	Acid density = 0.75 mmol/g Total acid density = 3.01 mmol/g BET area = 468 m^2/g Average pore diameter = 4.0 nm Total pore volume = 0.39 cm^3/g	Feedstock = Oleic acid Alcohol:oil 20:1 Time = 10 hours Temperature = 64 °C Loading = 3 wt%	TOF = 102.3 h^{-1}	Maintain high conversion at above 50 % after 3 cycles	Konwar, et al. (2015)
Direct sulphonation with H_2SO_4		Acid density = 0.30 mmol/g Total acid density = 2.01 mmol/g BET area = 690 m^2/g Average pore diameter = 4.1 nm Total pore volume = 0.61 cm^3/g		TOF = 26 h^{-1}	Conversion decreases immensely after 3 cycles	
Hydrothermal sulphonation with H_2SO_4		Acid density = 1.30 mmol/g Total acid density = 4.2 mmol/g BET area < 1 m^2/g		TOF = 29.2 h^{-1}	Conversion maintained at about 40 % after 3 cycles	

Table 2.4: (continued)

Sulphonation method	Carbon source	Catalyst Characterisation	Esterification & Transesterification conditions			Reference
			Operating conditions	Yield(Y)/ Conversion (C)/ Turnover frequency (TOF)	Recyclability	
Functionalisation with p-toluenesulphonic acid	*C. inophyllum* seed cake	Acid density = 0.03 mmol/g Total acid density = 1.0 mmol/g BET area = 0.7 m^2/g	Feedstock = *C. inophyllum* oil Alcohol:oil 20:1 Time = 10 hours Temperature = 64 °C Loading = 3 wt%	C = 74.3 % Y = 10.3 %	-	Dawodu, et al. (2014)
Direct sulphonation with concentrated H_2SO_4		Acid density = 0.8 mmol/g Total acid density = 2.9 mmol/g BET area = 0.8 m^2/g		C = 87.2 % Y = 75.0 %	Yield decreased by 67.6 % after 5 cycles	
In-situ polymerisation of acetic anhydride and sulphuric acid	Multi-walled carbon nanotubes (MWCNT)	Acid density = 0.30 mmol/g	Feedstock = Palm fatty acid distillate Alcohol:oil 20:1 Time = 3 hours Temperature = 170 °C Loading = 2 wt%	Y = 85.8 %	Yield maintained above 70 % after 5 cycles	Shuit and Tan (2014)
In-site polymerisation of poly(sodium 4-styrenesulphonate)		Acid density = 0.061 mmol/g		Y = 93.4 %		
Thermal decomposition of ammonium sulphate		Acid density = 0.029 mmol/g		Y = 88.0 %		

2.4.2 Factors Affecting Attachment of Active Groups

Subsection 2.2 has compared the effectiveness of using carbon-based solid acid catalyst in place of metal-based SACs as it is the cheaper alternative, and provides equally (and even higher) biodiesel yield. The attachment of the functionalised group, $-SO_3H$ during sulphonation is important to ensure the catalyst produced has a dense acid site to provide high conversions during both esterification and transesterification. The types of carbon precursor used, carbonisation time, carbonisation temperature and even sulphonation temperature can affect the structure of the carbonised material produced, which in turn affects the integration of the $-SO_3H$ groups during sulphonation.

2.4.2.1 Types of Raw Material

It has been referenced repeatedly that the performances of these unique catalysts is significantly reliant on the raw material used for their synthesis. For example, the sugar catalyst derived from D-glucose gave a favourable yield in its catalysis; however, similarly sulphonated catalysts prepared from incompletely carbonised resins, amorphous carbon, activated carbon and natural graphite exhibited no improvement in catalytic activity (Konwar, et al., 2014).

Lou, et al. (2008) had showed the effect of different starting materials had on the esterification and transesterification of biomass. All the carbohydrate-precursors – starch, cellulose, sucrose and D-glucose – were carbonised and directly sulphonated using concentrated H_2SO_4. The starched-derived catalyst had the highest activity among the four, and achieved this milestone in the shortest duration of 3 h. Elementary analysis (EA) and X-ray photoelectron spectroscopy (XPS) results indicated that the starch-derived SAC was composed of polycyclic aromatic carbon rings oriented in a random fashion, and had the highest $-SO_3H$ group densities than its counterparts, despite them all having small surface areas. In addition, it clearly had larger BET surface area, pore size, pore volume and a more hydrophobic surface than the three other starting materials (Lou, et al., 2008).

Lou, et al. (2008) further inferred that the high acid site densities were attributed to the attachment of the active group not only on the catalyst surface but within the amorphous carbon bulk. The relatively larger pore size and pore volume of the sulphonated starch catalyst in comparison with the three other carbohydrates increased the accessibility of reactants into the bulk to reach the $-SO_3H$ sites. Chen

and Fang (2011) also produced a saccharide-based catalyst and found that the amylopectin content in starch disturbed the PAH structure which was important for the attachment of $-SO_3H$ groups.

The catalyst derived from vegetable oil asphalt by Shu, et al. (2009) was a flexible material composing of sulphonated PAHs, which can exert an electron-withdrawing force on the hydrogen-bonded sulphonic groups, improving $-SO_3H$ stability. Furthermore, the asphalt had loose irregular networks and part of the particles had agglomerated. After sulphonation treatment by concentrated H_2SO_4, the scanning electron microscope (SEM) images showed that the agglomerates had fragmented to a certain degree with increase in pore size. The disintegration of the agglomerates likewise suggested that the synthesised catalyst had a high density of acid sites on the external surface, which were readily available to the reactants.

SEM images by Ezebor, et al. (2014) revealed the properties of raw oil palm trunk and sugarcane bagasse that could improve or obstruct the sulphonation process (Figure 2.3). Contrary to oil palm trunk, the sugarcane bagasse had a flake-like structure, signifying that the phenolic groups were easier to access than the SO_3H groups, accounting for its lower acid site density and slightly lower catalyst activity. Besides, the *C. inophyllum* seed cake-based catalyst synthesised by Dawodu, et al. (2014) showed high number of smaller carbon sheets, which in turn yielded high $-SO_3H$ densities, but the activity of the catalyst decreased drastically after the fifth cycle due to leaching. This was attributed to the weak bonding between the small carbon sheets and the active group.

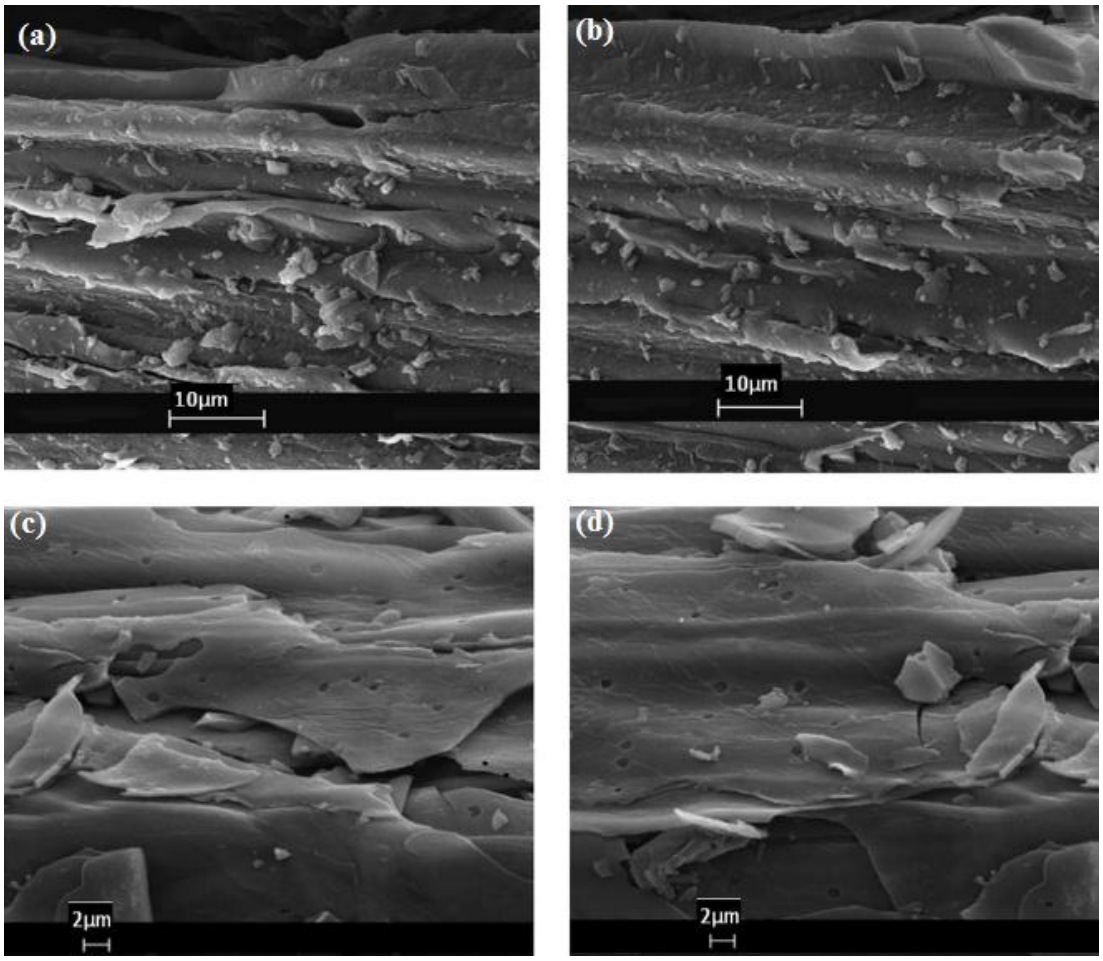

Figure 2.3: SEM Images of Raw Oil Palm Trunk (a) and (b); and Raw Sugarcane Bagasse (c) and (d) (Ezebor, et al., 2014)

Konwar, et al. (2015) had also demonstrated the variations in $-SO_3H$ densities for the sulphonated de-oiled waste cake (DOWC) derived from different materials. The study showed that $-SO_3H$ density increased with increasing carbon content in the activated carbon due to the increase in availability of the aromatic carbon sheets for attachment. Although, in the study conducted by Geng, et al. (2011), increasing carbon content of carbon-coated alumina (CCA) created larger and thicker carbon sheets joined to form a continuous framework, rendering it less soluble due to the rigid framework formed. Therefore, although most of the CCA samples had high acid site densities, BET area and pores, rising carbon content lowered the turnover frequency as the catalyst became increasingly insoluble in polar solvents.

2.4.2.2 Carbonisation Temperature

As mentioned in Sub-subsection 2.3.2, Lou, et al. (2008) had showed that increasing carbonisation temperatures improved catalytic performance but only up to a certain temperature before performance declines. It was deduced that samples carbonised at lower temperatures (< 648 K) had a higher phenolic −OH density, thus additional water produced from esterification can be adsorbed onto the catalyst surface, making it more hydrophilic, therefore impeding the access of the relatively hydrophobic fatty acids or triglycerides to the catalyst.

Furthermore, the sample produced at low carbonisation temperature (< 648 K) was a soft aggregate that comprised of $-SO_3H$ groups attached onto small polycyclic aromatic carbon sites rather than a rigid carbon material, which can be readily leached at high temperatures or in the presence of higher amount of fatty acids due to the weaker bonding. On the other hand, carbonisation at higher temperatures (> 648 K) would make the carbon structure more rigid, presumably due to the growth and stacking of large polycyclic aromatic carbon sheets, resulting in a catalyst with lower flexibility and reduced surface area for $-SO_3H$ attachment, thereby leading to a lower acid site density (Lou, et al., 2012).

2.4.2.3 Carbonisation Time

In Sub-subsection 2.3.2, various studies had shown that increasing carbonisation time increased the catalytic performance but only up to a certain duration before conversion plummeted (Mo, et al., 2008; Lou, et al., 2008). The study carried out by Dawodu, et al. (2014) further supported the findings made by Mo, et al. (2008) regarding the effect of carbonisation time on catalytic performance. As mentioned before, the acid density results demonstrated that the catalyst prepared from materials carbonised for 1 h possessed more small carbon sheets and hence higher SO_3H densities than the catalyst derived from material carbonised for 5 h (Dawodu, et al., 2014).

The study conducted by Borhan and Kamil (2012) illustrates the development of the surface morphology of rubber seed shell with increasing carbonisation time, providing an idea of the effect of carbonisation duration on catalyst porosity. The shell was carbonised at a fixed temperature of 500 °C, and the SEM images showed that the surface structure of the raw material differed greatly to that of the activated carbons (Figure 2.4). Figure 2.4 (b) shows the formation of canal structures,

indicating that the material was still undergoing the early stages of carbonisation. Large pores were clearly found on the activated carbon surface, leading to high surface area and porosity.

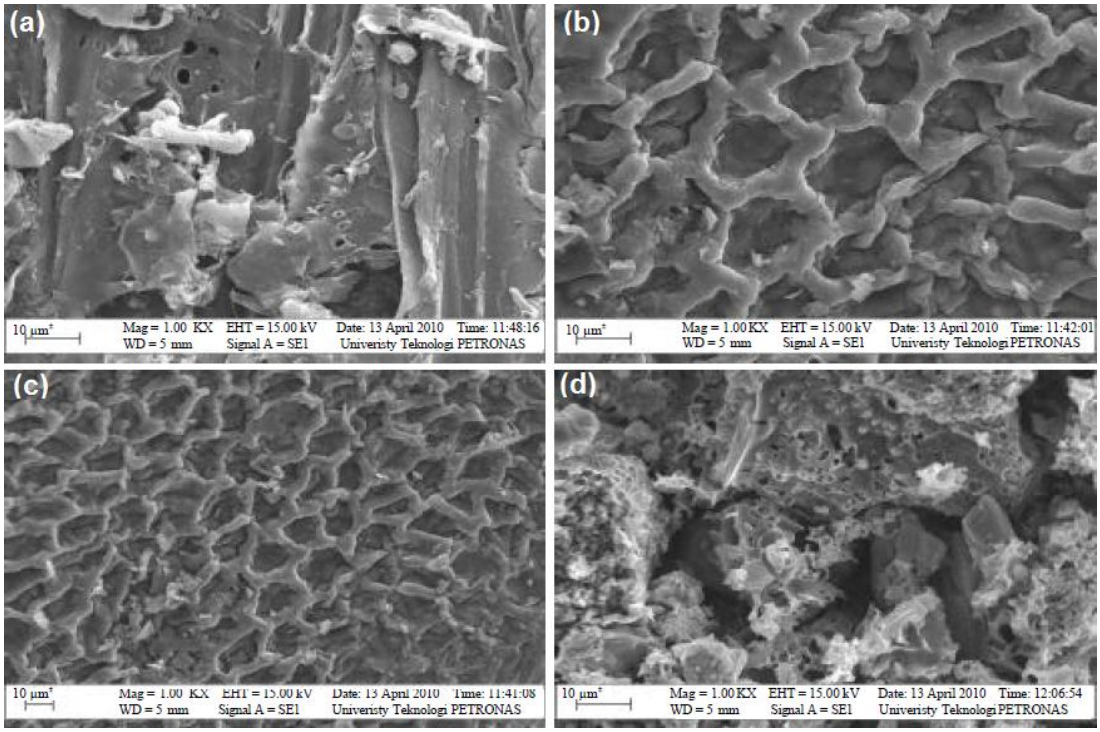

Figure 2.4: SEM Images of (a) Raw Rubber Seed Shell; (b) Activated Carbon at t = 0.5 h; (c) Activated Carbon at t = 2.5 h and (d) Activated Carbon at t = 3 h. All biomass were carbonised at 500 °C. (Borhan and Kamil, 2012)

Continual carbonisation up to 2.5 h under the same carbonisation temperature of 500 °C causes the canal structure to be broken down, where the activation process had occurred, leading to the formation of more canals, which was considered a good surface texture and enabled activating agents to enter the bulk of the activated carbon. At 3 h of carbonisation, Figure 2.4 (d) provided the highest BET surface area with the most well-developed porous structure. Hence, the acid site density should increase with increasing carbonisation duration as porosity increased, which in turn led to a higher biodiesel yield.

2.4.2.4 Sulphonation Temperature

Although not much work was done on the effect of sulphonation time and temperature, Lou, et al. (2012) had found that as sulphonation temperature increased (373 to 423 K in this study), the resulting catalyst showed a marked enhancement in esterification and transesterification activities (Figure 2.5). However, further temperature increment above 423 K led to a rapid drop in activity. On the other hand, the FAME yield for both esterification and transesterification increased favourably with increasing sulphonation time until it reached maximum yield at 15 h of sulphonation. Fourier Transform-Infrared Spectroscopy (FT-IR) spectra of the carbonised carbon precursors in Figure 2.6 showed that the peak intensity due to C=O groups at 1710 cm^{-1} was greatly enhanced, whereas the peaks for aliphatic C-H at about 1610 cm^{-1} diminished once sulphonation was carried out. This showed that besides the integration of $-SO_3H$ groups, sulphonation also resulted in structural changes, and this was highly dependent on sulphonation temperature.

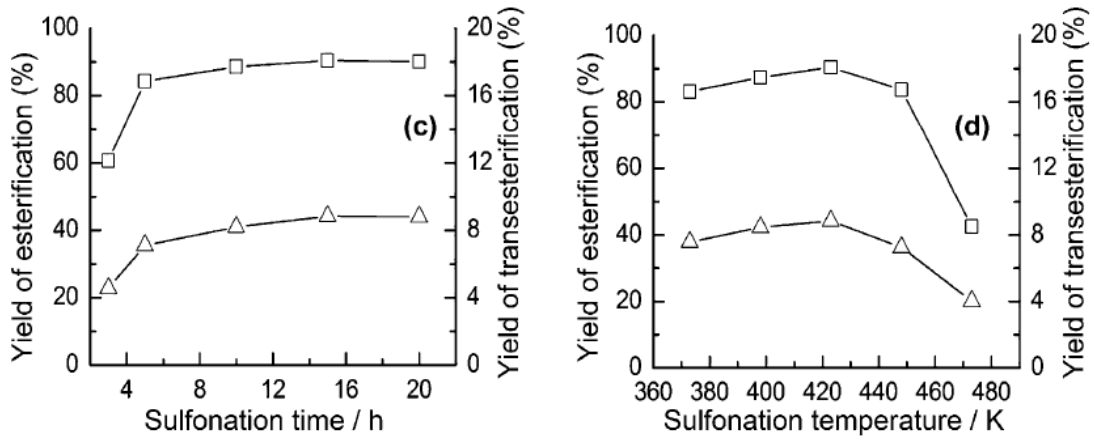

Figure 2.5: Influence of Sulphonation Conditions on Esterification (□ and striped bars) and Transesterification (∆ and black bars) Activities of Bagasse-Derived Catalysts (Lou, et al., 2012)

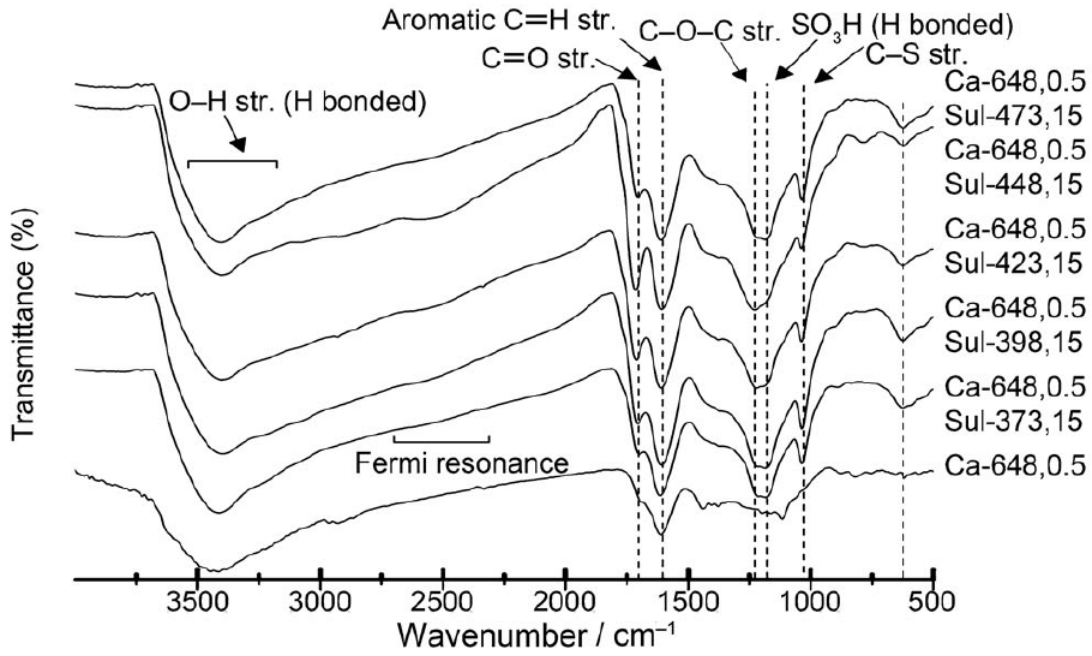

Figure 2.6: FTIR Spectra on the Effect of Varying Sulphonation Temperatures (373 – 473 K) (Lou, et al., 2012)

Overall, 4-BDS is a better sulphonation method as it is more environmentally benign; it is able to sulphonate more rigid, ordered carbon structures and provides higher acid densities. Carbon is also a better choice in catalyst synthesis as it provides the site of $-SO_3H$ attachment, although a balanced carbon content has to be reached whereby it contains enough sites for functionalization without rendering the catalyst insoluble in the reacting solvent. In addition, increased carbonisation temperature and duration will increase the acid site density, which in turn could improve the yield of biodiesel.

CHAPTER 3

METHODOLOGY AND WORK PLAN

3.1 Materials and Apparatus

3.1.1 Raw Material and Chemicals

Table 3.1 lists down the chemicals used in the carbonisation and sulphonation of rubber seed kernel, the chemicals involved in the esterification of palm fatty acid distillate and the characterisation of the catalyst and biodiesel. The rubber seed was supplied by a small rubber tree estate and the shell was a waste obtained when extracting the kernel.

Table 3.1: Raw Materials and Chemicals Used

Chemicals/Materials	**Source**	**Estimated amount**	**Usage**
Rubber seed	Rubber estate	Excess	Obtain shells to be used as carbon precursor to synthesise SAC
Distilled water	UTAR	Excess	To wash the materials and to sulphonate the biomass
85% phosphoric acid	UTAR	1.5 L	To activate biomass and sulphonate carbonized material
Sulphanilic acid	Chemolabs	200 g	To produce the sulphonating agent, 4-BDS
37% hydrochloric acid	UTAR	500 mL	To produce the sulphonating agent, 4-BDS and calculate the acid site density of SAC

Table 3.1: (continued)

Chemicals/Materials	**Source**	**Estimated amount**	**Usage**
Sodium nitrite	Chemolabs	100 g	To produce the sulphonating agent, 4-BDS
98% Ethanol	UTAR	1 L	To produce the sulphonating agent, 4-BDS
Palm fatty acid distillate (PFAD)	UTAR	Excess	Reactant in esterification to produce biodiesel
99% Methanol	UTAR	2.5 L	Reactant in esterification to produce biodiesel
1 M Potassium Hydroxide	UTAR	20 mL	To measure the acid value of FAME by titration
Isopropanol	UTAR	500 mL	To dissolve FAME produced for titration
Hexane	UTAR	10 mL	To dissolve biodiesel for GC analysis
0.1 M Sodium hydroxide	UTAR	4 g	To measure the acid site density of SAC
Phenolphthalein	UTAR	100 mL	As an indicator in back titration and titration

3.1.2 Apparatus and Equipment

Table 3.2 shows the apparatus and equipment utilized in the carbonisation and sulphonation of the rubber seed shells, and the esterification of PFAD.

Table 3.2: Apparatus and Equipment Used

Apparatus/Equipment	Specifications	Usage
Oven	80 °C, overnight	To dry the washed biomass, carbonized and sulphonated material
Carbolite furnace	Carbolite RHF 15/8	To carbonize the activated rubber seed shells
Buchner funnel and pump	90 mm	To filter out carbonized and sulphonated material from filtrate
Blender	-	To blend raw rubber seed shells into smaller size
Mortar and pestle	-	To grind activated carbon produced
Sieve	ASTM no.60 sieve	To ensure activated carbon are of a uniform size of 250 µm
Ice water bath	2 L	To produce 4-BDS
Coiled condenser	29/32	To condense methanol vapours during esterification
Heating mantle	-	To heat and stir the esterification mixture
Hot plate stirrer	-	To stir the sulphonation mixture

3.1.3 Instruments

Table 3.3 below provides an overview of the instruments that are utilized in the catalyst and biodiesel characterisation, the respective models and specifications, and their functions in characterising catalyst and biodiesel.

Table 3.3: Instruments Used for Catalyst and Biodiesel Characterisation

Instrument	Specification	Function
Scanning Electron Microscopy (SEM)	Hitachi S-3400N	To analyse surface topography, morphology crystalline structure and orientation of catalyst
Sorptomatic Surface Area Analyser (BET)	Thermo Scientific SO1990	To measure the total specific surface area of the catalyst.
Electron Dispersive X-Ray Spectroscopy (EDX)	-	To identify the chemical elements and their respective concentrations in the catalyst.
X-Ray Diffractometer	Shidmazu XRD-6000	To determine the crystal structure of the catalyst.
Fourier Transform Infrared Spectroscopy (FT-IR)	Nicolet IS10	To identify the functional groups present in the catalyst.
Thermogravimetric Analysis (TGA)	-	To analyse the thermal stability of the components in the catalyst.

3.2 Research Methodology

Figure 3.1 below shows the overall summarized methodology that will be the basis for this research in determining the optimal carbonisation time, amount of sulphonating agent:activated carbon ratio, esterification duration and esterification temperature.

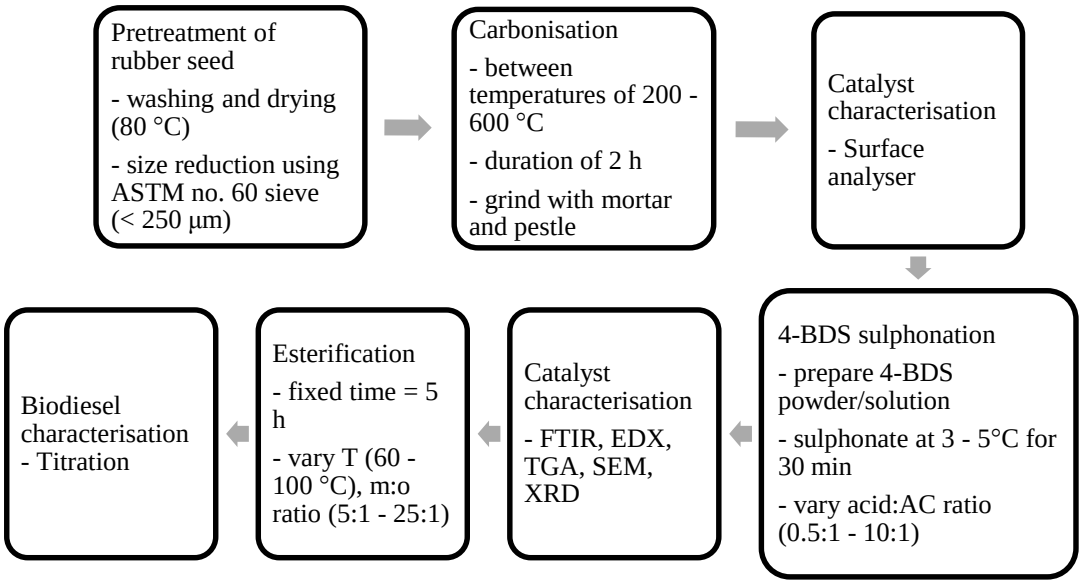

Figure 3.1: Process Flow of Research Procedure

3.3 Experimental Procedures

3.3.1 Carbonization of Biomass to Form Activated Carbon (AC)

The rubber seed shells were first washed to remove any dirt or impurities before placing in an oven for 24 h at 80 °C to remove moisture completely (Figure 3.2). The shells were then blended and crushed into smaller pieces of about 850 μm. The crushed shells were then presoaked with 30% (v/v) phosphoric acid in 2:1 w/w impregnation ratio for 24 hrs at room temperature as shown in Figure 3.3. The material was then washed thoroughly with distilled water and dried in an oven overnight. The dried solids were then transferred into a 100 mL silica crucible with lid and carbonized in a furnace at temperatures ranging from 200 °C to 600 °C for 2.5 h (Figure 3.4). The black carbonized solid produced was then cooled to room temperature before being grounded and sieved with an ASTM no. 60 sieve to obtain average particle size of < 250 μm (Figure 3.5).

The activated carbon samples carbonized between temperatures of 200 to 600 °C were named AC200, AC300, AC400, AC500 and AC600 accordingly as shown in Table 3.4. Catalyst characterisation was performed to find the most optimal surface area before the most suitable AC sample was chosen to undergo sulphonation.

Figure 3.2: Washed Rubber Seed Shells

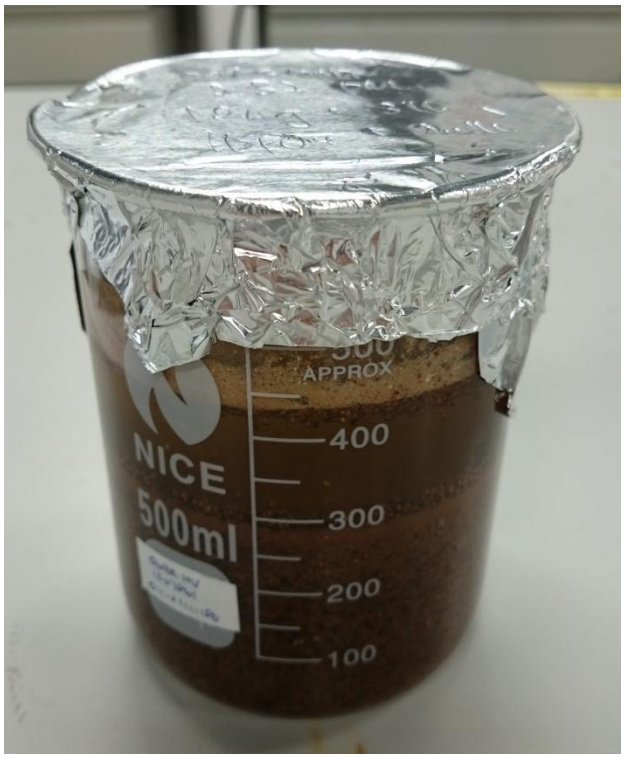

Figure 3.3: Crushed Rubber Seed Shells Presoaked in 30 % v/v H_3PO_4

Figure 3.4: Presoaked Rubber Seed Shells in a Carbolite Furnace

Figure 3.5: Carbonised Material Being Grinded

Table 3.4: Carbonisation Parameters and AC Nomenclature

Carbonisation Temperature	**After Carbonisation**
200 °C	AC200
300 °C	AC300
400 °C	AC400
500 °C	AC500
600 °C	AC600

3.3.2 Functionalisation of AC by 4-Benzenediazoniumsulphonate

6 g of sulphanilic acid was dispersed in 300 mL of 1M HCl aqueous solution in a round bottomed flask. The flask was then submerged into an ice bath with temperatures maintained at 3-5 °C with continuous stirring. 90 mL of 1M $NaNO_2$ aqueous was then added dropwise and a clear solution was obtained. After 1 h of stirring at the same temperature, the white precipitate of 4-BDS formed was filtered off, washed with distilled water before being transferred to a 500 mL beaker containing 200 mL of distilled water and 60 mL of ethanol. Then, 3.0 g of the AC sample was added into the beaker and the temperature maintained at 3-5 °C, followed by the subsequent addition of 100 mL of 30-32% H_3PO_4 aqueous solution. After 30 min of stirring, another 50 mL of H_3PO_2 was added and the mixture was allowed to stand for 1 h with occasional stirring. The sulphonated AC produced was then washed intensively with distilled water before being dried in a vacuum overnight. The setup of the experiment is shown in Figure 3.6.

The sulphonation procedure was repeated on the AC with the most promising surface area for different sulphanilic acid to AC ratios – 2:1; 4:1; 6:1; 7:1, 8:1 and 10:1. Catalyst characterisation was once again carried out to find the optimal sulphanilic acid to AC ratio before the most desirable catalyst was used to carry out the esterification process. The parameters investigated and the nomenclatures of the catalysts produced are shown in Table 3.5.

Figure 3.6: Experimental Setup for Sulphonation of AC

Table 3.5: Carbonisation and Sulphonation Parameters and Catalyst Nomenclature

Sulphanilic Acid to Activated Carbon Ratio	**After Sulphonation**
2:1	SAC2:1
4:1	SAC4:1
6:1	SAC6:1
7:1	SAC7:1
8:1	SAC8:1
10:1	SAC10:1

3.3.3 Catalytic Tests

Once the sulphonated catalyst with the highest acid density was determined, the SAC produced was used to catalyse the esterification and transesterification of palm fatty acid distillate (PFAD) to biodiesel. The esterification procedure was carried out in a 250 mL round bottom flask equipped with a magnetic stirrer and heating mantle with temperatures kept constant at 90 °C. 3 wt% (0.3 g) of the chosen SAC catalyst was added to appropriate amounts of methanol (15:1 molar ratio), stirred and heated to 90 °C before 10.0 g of PFAD was added with vigorous stirring at 300 rpm for 2.5 h. The setup of the apparatus for esterification is shown in Figure 3.7. Once the reaction was completed, the catalyst was filtered out and excess methanol was evaporation. The esterification process was repeated for various parameters shown in Table 3.6.

Table 3.6: Esterification Parameters

Esterification Parameters	**Variables**
Methanol to oil ratio	5:1, 10:1, 15:1, 20:1, 25:1
Esterification duration	3 h, 4 h, 5 h, 6 h, 8 h

Figure 3.7: Experimental Setup for Esterification of PFAD

3.4 Catalyst Characterisation

Once the solid acid catalyst was synthesised, numerous instruments were utilised in its characterisation. The Brunauer-Emmett-Teller (BET) surface analyser, scanning electron microscope (SEM), electron dispersive x-ray spectroscopy (EDX), Fourier

Transform-infrared spectroscopy (FT-IR), thermogravimetric analysis (TGA), x-ray diffraction (XRD) and the acid density test were used to better understand the structure, morphology, composition, and thermal stability of the catalyst.

3.4.1 Scanning Electron Microscopy (SEM)

The SEM focuses high-energy electrons into a beam to generate a variety of signals on the surface of the solid specimen. The interactions between the beam of electrons and the sample produce signals that reveal information on surface morphology, chemical composition, crystalline structure and orientation of materials making up the sample (Swapp, 2017). High resolution images are routinely generated to show the topography of the sample.

3.4.2 BET Surface Area Analyser

The Brunauer-Emmett-Teller (BET) surface analyser provides specific surface area evaluations via nitrogen sorption analysis. Nitrogen adsorption and desorption curves are obtained before the BET theory is utilized to calculate the total specific surface area in units of m^2/g; the total specific surface area encompasses the external area and pore area evaluations (HORIBA, 2017).

Once the catalysts surfaces have been analysed and the catalyst with the most ideal surface chosen (polycyclic aromatic carbon sheets with high pore volume, pore size and large surface area), the activated carbon was then sulphonated with 4-BDS for SO^3H group attachment. Further characterisation of the synthesized solid acid catalyst were carried out using Electron Dispersive X-Ray Spectroscopy (EDX), Fourier Transform Infrared Spectroscopy (FT-IR) and Thermogravimetric Analysis (TGA) to analyse the presence of the acid group and its densities, and the thermal stability of the catalyst.

3.4.3 Electron Dispersive X-ray Spectroscopy (EDX)

Electron dispersive spectrometry utilizes the x-ray spectrum emitted by the sample when it is bombarded with a beam of electrons. Elemental compositions can be analysed as in principle, all elements from atomic number 4 (Be) to 92 (U) can be detected. Each element gives out a specific emission spectra with the concentrations measured according to the line intensities and comparing with a standard (University of California, 2016).

3.4.4 Fourier Transform – Infrared Spectroscopy (FT-IR)

FT-IR involves the study of the interactions between the sample and the electromagnetic fields in the infrared region to identify organic and inorganic materials. A material irradiated with IR radiation excites molecules to a higher vibrational and rotational state. The wavelengths of light adsorbed are characteristic of a particular functional group. The signal obtained from the detector is a combination of constructive and destructive interferences, which is analysed by the computer to give a single-beam IR spectrum for functional group analysis (Materials Evaluation and Engineering, Inc., 2017).

3.4.5 Thermogravimetric Analysis (TGA)

TGA analysis measures the mass of a substance against time as the sample is subjected to heat. In other words, the weight of the sample would increase or decrease upon heating. The measurements obtained are primarily used to determine the composition of materials present and also to predict their thermal stability. It characterizes materials according to the weight lost or gained from the decomposition, oxidation and reduction of the compounds (Perkin Elmer, 2015).

3.4.6 X-ray Diffraction (XRD)

X-ray diffraction is a method of determining the arrangement of atoms within a crystal. Solid matter can be described as either amorphous or crystalline. An alternating electromagnetic field (x-ray) is applied to the sample. When this beam hits an atom, the electrons surrounding the atom will oscillate at the same frequency as the field. Both constructive and destructive interference are observed, but only waves which are in phase (constructive) are detected by the detector to produce an XRD spectrum as no resultant energy is produced from destructive waves. By studying the detector angle in the form of 2θ, the shape of the unit cell can be found, and hence the dimension of the unit cell can be calculated. (Thermo ARL, 1999)

3.4.7 Acid Density Test

The acid density test is a practical mean of finding the total acid density of the sulphonated material. It applies the principle of titration and is also called back titration. For this experiment, 0.04 g of sample was added to 0.01 M NaOH solution

and mixed well for 30 minutes. The solid sample was then filtered out and the filtrate was titrated with 0.01 M HCl using phenolphthalein as an indicator. The volume of HCl used corresponds to the number of moles of NaOH molecules left unreacted within the filtrate. By calculating the number of moles of NaOH neutralised, the total acid density of the sample may be found. (Fu, et al., 2015; Liu, et al., 2013; Malins, et al., 2015).

3.5 Biodiesel Characterisation

Back titration was carried out on the biodiesel obtained from the esterification process in order to determine the conversion of free fatty acids (FFA) contained within the PFAD.

3.5.1 Back Titration

Back titration is normally carried out to find the concentration of FFA, or the acid number of biodiesel. Biodiesel are usually produced via esterification or transesterification which uses high FFA source as precursors. In this study, the initial acid value of the PFAD was first determined. Once esterification is completed, the acid value of the oily product was found before subtracting this value with the initial acid value to find the number of free fatty acid molecules neutralised. This can then be compared with the initial acid value to find the conversion.

Blank titration was first carried out by neutralising 10 mL of isopropanol with 0.1 M KOH solution using phenolphthalein as an indicator. As isopropanol was used to dissolve the biodiesel sample, carrying out the blank titration ensures that the number of KOH molecules neutralised by the isopropanol is excluded from the final calculation. 1 g of biodiesel sample was then dissolved in 10 mL of isopropanol and once more titrated with 0.1 M KOH solution with phenolphthalein acting as an indicator. End point of titration was obtained once the solution reached a permanent reddish-orange colour. The acid number was then calculated based on Eq. (3.1):

$$AV(mg\ KOH^{-1}) = \frac{56.1 \times M \times V}{W} \tag{3.1}$$

Where

M = molarity of the solution, M

V = volume of KOH reacted, cm^3

W = the weight of the sample, g

CHAPTER 4

RESULTS AND DISCUSSION

4.1 Introduction

In this report, a total of four different parameters were studied. The first parameter involved the temperature of carbonisation of the rubber seed shells, from a temperature of 200 °C to 600 °C. The second parameter studied the sulphanilic acid:activated carbon ratio (acid:AC ratio) during sulphonation, ranging from 2:1 to 10:1. Once the most optimal value for both the carbonisation temperature and acid:AC ratio were chosen, the solid acid catalyst (SAC) produced was used in the production of biodiesel from palm oil fatty distillate (PFAD).

The third and fourth parameters studied the effects of methanol:oil ratio (from 5:1 to 25:1) and duration (3 h to 8 h) on esterification and transesterification in producing biodiesel. The conversion of PFAD into biodiesel and its yield were investigated and characterised.

4.2 Catalyst Characterisation

The rubber seed shells were carbonised at temperatures ranging from 200 °C to 600 °C to study the effect of carbonisation temperature on the surface morphology of the activated carbon produced, and more importantly, the specific surface area. The temperature increment was 100 °C. About 0.5 g of black powder produced was then analysed using the Sorptomatic Surface Area Analyser using the Brunauer-Emmett-Teller (BET) equation to find the respective specific surface areas. The surface morphologies of the carbonised rubber seed shells were analysed using scanning electron microscopy (SEM), at a magnification of 6,000.

The AC produced at carbonisation temperatures of 200 °C, 400 °C and 600 °C were taken to be analysed. The results obtained from the surface analyser were tabulated in Table 4.1 and plotted in Figure 4.1.

Table 4.1: Specific Surface Area and Pore Specific Volume at Different Carbonisation Temperatures

Sample	Carbonisation temperature (°C)	Specific surface area (m^2/g)
AC200	200	0.6560
AC400	400	3.470
AC600	600	238.0

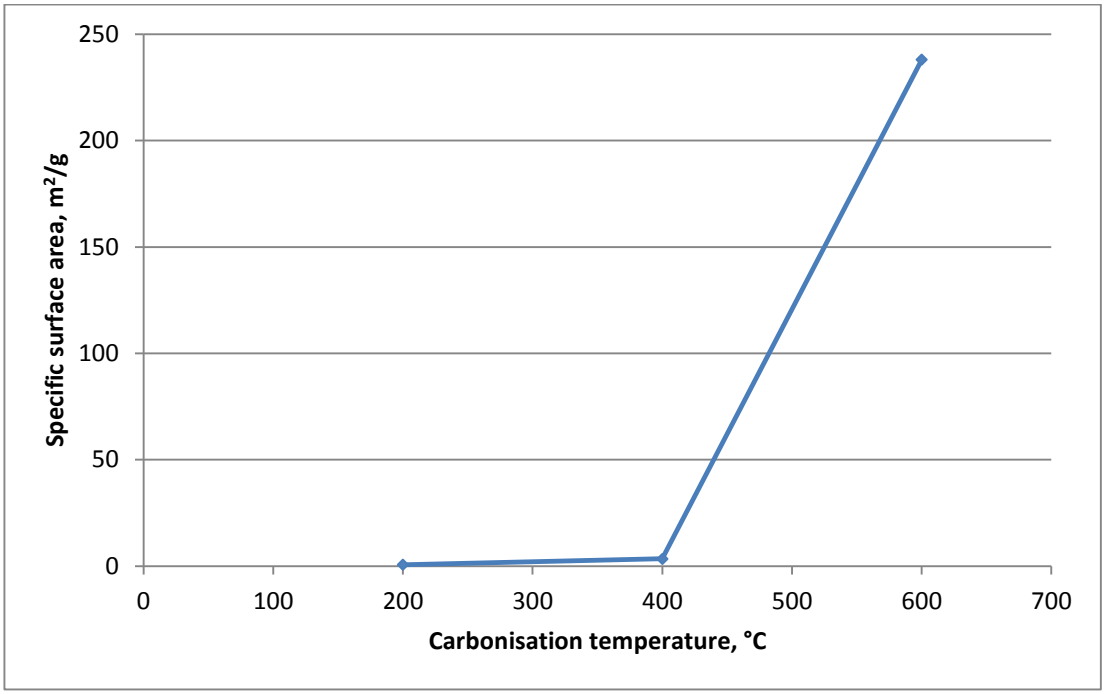

Figure 4.1: Graph of Specific Surface Area against Carbonisation Temperature

Figure 4.1 shows that the specific surface area gradually increased from 0.6560 m^2/g to 3.470 m^2/g as the carbonisation temperature was raised from 200 °C to 400 °C, before increasing steeply to 238 m^2/g from 400 °C to 600 °C. The slight increment in specific surface area from 200 °C to 400 °C could be due to insufficient heat provided to remove the volatile compounds and develop rudimentary pores (Borhan and Kamil, 2012). Besides that, the phosphoric acid used might be too weak to aid in the chemical activation of rubber seed shells as literatures such as Pangketanang, et al. (2015) and Borhan and Kamil (2012) used the stronger base, KOH to activate the rubber seed shells. The steep rise in specific surface area from 400 °C to 600 °C can be explained by the increase in heat energy to enhance the removal of volatile compounds from the rubber seed shell (Borhan and Kamil, 2012).

The SEM images in Figure 4.2 helped illustrate this pore formation. Before carbonisation, the surface of the rubber seed shells was smooth with no pores (Figure 4.2 (a)). When the raw material was carbonised at 200 °C, it can be seen in Figure 4.2 (b) that the surface of the shell has started to disintegrate, producing a specific surface area of 0.6560 m^2/g. As the carbonisation temperature was increased to 400 °C, small pores had developed with an average pore diameter of 0.5 μm, raising the specific surface area to 3.470 m^2/g (Figure 4.2 (c)). Once more, according to Borhan and Kamil (2012), this was because more heat was provided to further disintegrate the organic structure, increasing the carbon content, widening the pore size. A further increase in temperature up to 600 °C not only increased the number of pores, but further expanded the pore diameter to 1.5 μm.

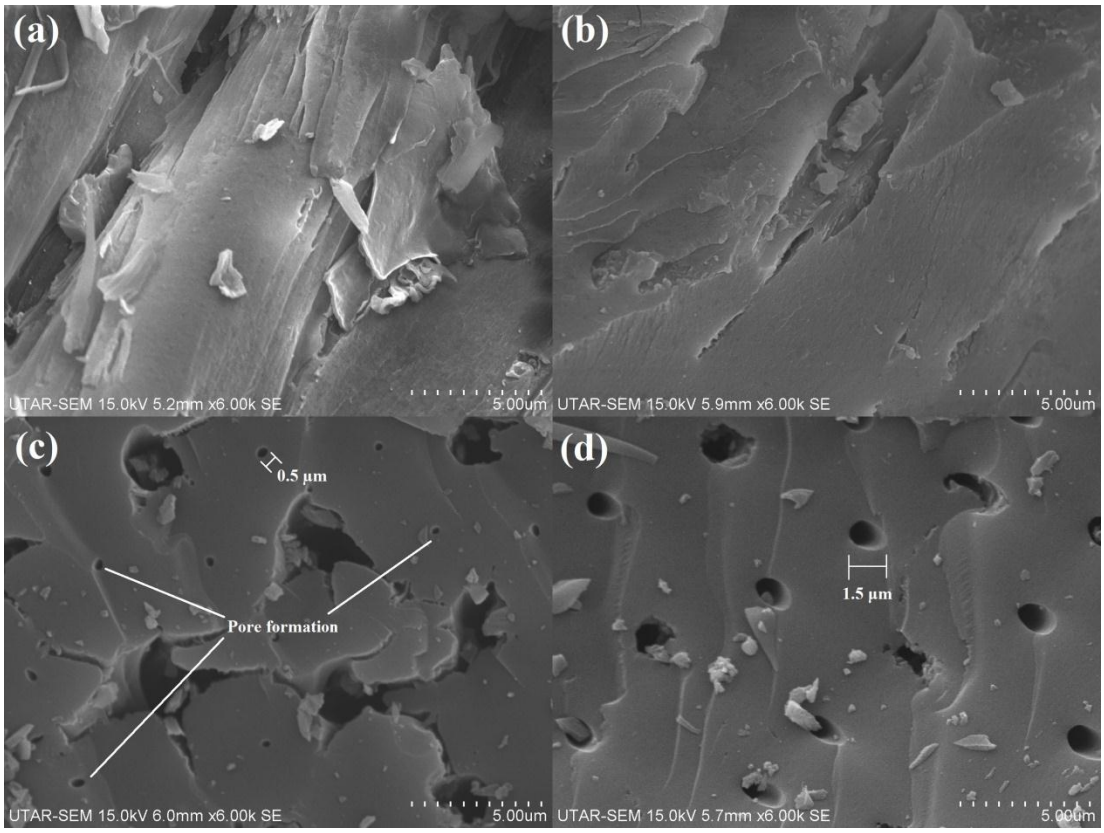

Figure 4.2: SEM images of (a) raw rubber seed shell, (b) AC200, (c) AC400 and (d) AC600

Therefore, it can be concluded that as carbonisation temperature was increased, the specific surface area of the activated carbon produced also increased. This was consistent with the findings done by Pangketanang, et al. (2015) whereby

the surface area of the carbonised rubber seed shells increased from 429 m^2/g to 620 m^2/g when it was carbonised from 700 °C to 900 °C. The results can further be supported by Geng, et al. (2012), which showed that increasing the carbonisation temperature increased the surface area of the sucrose-Al_2O_3 composite. Moreover, the results showed that between carbonisation temperatures of 200 °C to 600 °C, 600 °C was the most optimal carbonisation temperature. Any temperatures higher than 600 °C were not tested as according to Lou, et al. (2012), high carbonisation temperatures could cause the catalyst to be too rigid, and contain less SO_3H groups. Hence, the AC produced from 600 °C was chosen to undergo sulphonation.

Sulphonation of AC600 was carried out at varying sulphanilic acid amounts to investigate the effect of acid:AC ratio on the total acid density of the solid acid catalyst (SAC) synthesised via 4-benzenediazonium sulphonate (4-BDS) functionalisation. For this parameter, the sulphanilic acid:AC ratio was studied based on a weight-to-weight basis. The ratios varied from 2:1, 4:1, 6:1, 7:1, 8:1 and 10:1. Electron Dispersive X-ray Spectroscopy (EDX) was carried out to determine the presence and concentration of the sulphur atoms from the SO_3H groups. The acid density test was used to determine the total acid density of the SACs produced. The incorporation of the SO_3H groups onto the catalyst was further analysed using FT-IR spectroscopy. Once more, the surface morphology of the solid acid catalyst was analysed using the SEM, at a magnification of 6,000. The thermal stability of the catalyst was investigated using thermogravimetric analysis (TGA) using N_2 gas and heated to 900 °C. The crystallinity of the novel catalyst was determined by X-Ray Diffraction (XRD).

An example of the EDX spectrum, using sample SAC2:1 is given as Figure 4.3. It can be seen that elemental carbon and oxygen were detected. This should come as no surprise as all activated carbons contain carbon (C) and oxygen (O). The presence of elemental phosphorus (P) was contributed by the phosphoric acid used in the chemical activation of the crushed rubber seed shells. Moreover, elemental sulphur (S) can be attributed to the sulphonation process. The outlier in this case, which was elemental aluminium (Al), could be present due to its transfer during the crushing and grinding phase of the activated carbons.

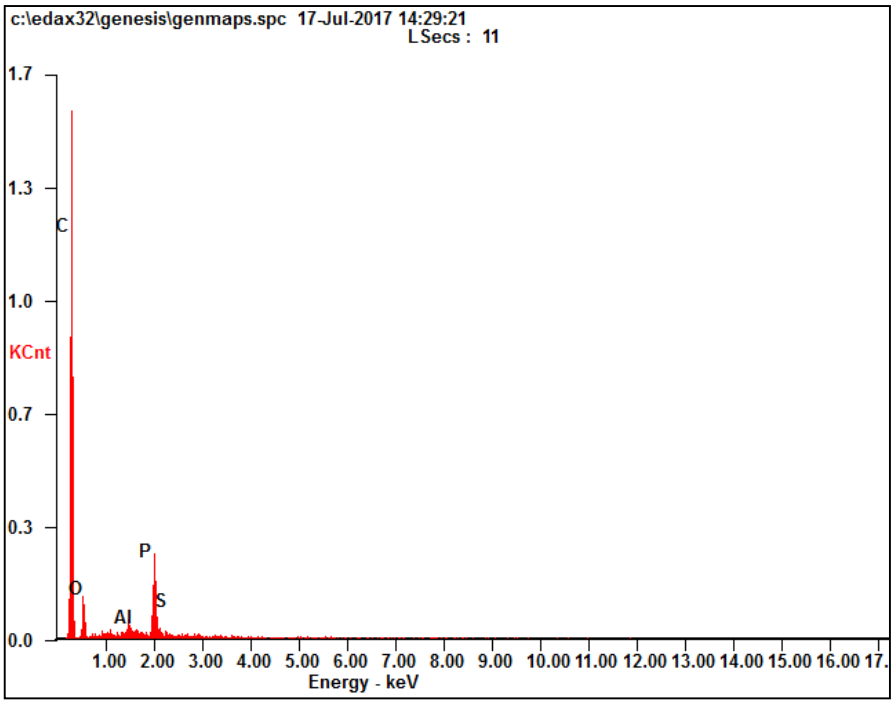

Figure 4.3: EDX Spectrum Showing the Elemental Compositions Within SAC2:1

The data acquired from the EDX elemental analysis was further tabulated into Table 4.2 whereas the data obtained from the acid density test was tabulated into Table 4.3. A graph of the elemental composition of sulphur (taking the highest value for each) and total acid density against acid:AC ratio was plotted in Figure 4.4.

Table 4.2: Elemental Sulphur Concentrations at Varying Sulphanilic Acid-to-AC Ratios

Sample	**Acid:AC ratio (w/w)**	**Elemental concentration of sulphur (wt%)**			
		Scanned area 1	**Scanned area 2**	**Scanned area 3**	**Average**
SAC2:1	2:1	0.00	0.25	0.34	0.20
SAC4:1	4:1	3.74	0.49	0.27	1.50
SAC6:1	6:1	9.03	8.89	3.75	7.22
SAC7:1	7:1	0.19	0.17	5.10	1.82
SAC8:1	8:1	0.00	0.92	0.92	0.61
SAC10:1	10:1	0.23	0.00	0.17	0.13

Table 4.3: Total Acid Density at Varying Sulphanilic Acid-to-AC Ratios

Sample	Acid:AC ratio (w/w)	Total acid density (mmol/g_{cat})
SAC2:1	2:1	2.325
SAC4:1	4:1	2.906
SAC6:1	6:1	2.894
SAC7:1	7:1	2.900
SAC8:1	8:1	2.694
SAC10:1	10:1	2.737

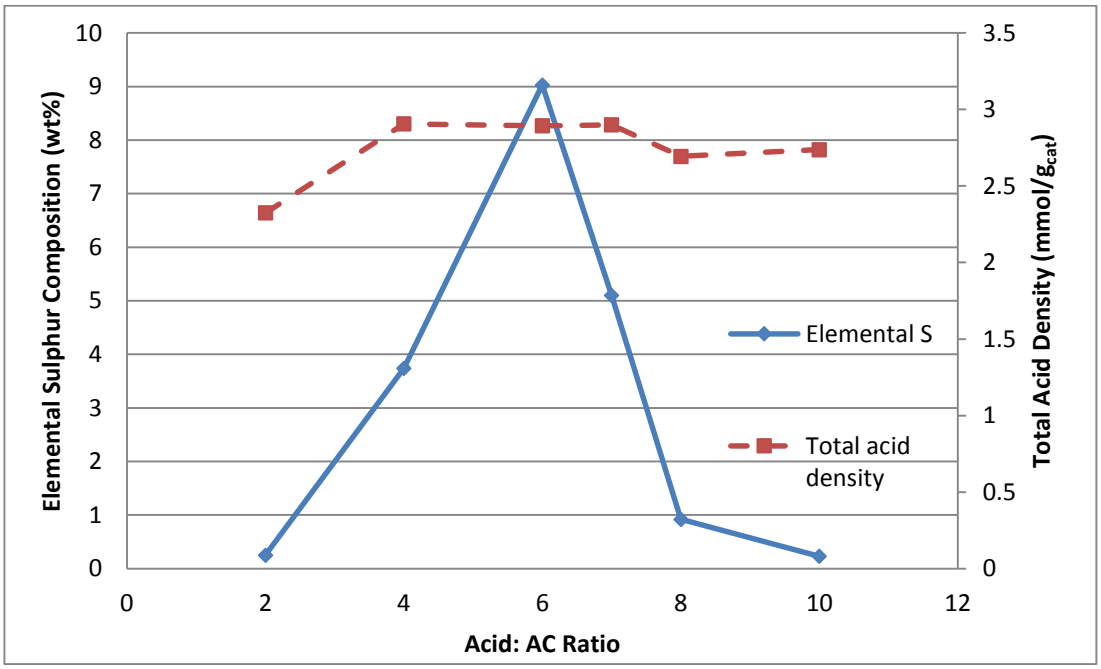

Figure 4.4: Graph of Elemental Sulphur Composition and Total Acid Density Against Sulphanilic Acid-to-Activated Carbon Ratio

Based on Figure 4.4, as the acid:AC ratio increased from a ratio of 2:1, the total acid density of the SAC produced increased, although this value reached a plateau of 2.906 mmol/g_{cat} at a ratio of 4:1 before decreasing to 2.694 mmol/g_{cat} at a ratio of 8:1. The initial increase was synonymous to the initial binding of the SO_3H groups to the surface of the carbonaceous material. As more 4-BDS was produced with increasing amounts of sulphanilic acid, more SO_3H groups were attached to the AC pores. The plateau could be explained whereby most of the binding sites in the mesopores and micropores developed during carbonisation had been fully occupied by the SO_3H groups. Besides, according to Konwar, et al. (2015), the amount of

sulphanilic acid caused minute changes to the catalyst's acid density as this depended on the sites available for SO_3H group attachments. The drop in acid density after ratio 8:1 could be due to the intensive washing of the catalyst as more washing cycles were needed to completely remove any unattached SO_3H groups. This could adversely cause some of the attached SO_3H groups to detach, subsequently lowering the total acid density.

It can be seen from Table 4.2 that the SAC with the most elemental sulphur present and with the best distribution was SAC6:1 – when the carbonised material AC600 was sulphonated with an acid:AC weight ratio of 6:1. Theoretically, it should have the highest acid density. However, according to Table 4.3, the catalyst with the highest acid density was SAC4:1. By comparing both the sulphur distribution and total acid density from Figure 4.4, SAC6:1 was chosen as the most promising solid acid catalyst to be used to synthesise biodiesel from PFAD. This was because although SAC6:1 has almost as high an acid density as that of SAC4:1, SAC6:1 has a better SO_3H group distribution (as indicated by EDX analysis) than SAC4:1. Its incorporation and distribution was shown in the SEM image on the right of Figure 4.6.

The FT-IR spectrum of the optimum catalyst produced was illustrated in Figure 4.5. The appearance of bands at 1099.48 cm^{-1} was attributed to S=O stretching whereas the band at 1272.75 cm^{-1} was due to SO_3H stretching as mentioned by Geng, et al. (2011) and Konwar, et al. (2014). Therefore, the presence of both bands in the FT-IR spectrum of the sulphonated AC600 signified the successful attachment of the SO_3H groups. On top of that, the presence of the weak acids were also indicated in the spectrum: the hydroxyl –OH group was characterised by the wavenumbers 3602.23 to 3852.80 cm^{-1} on the AC600 spectrum and 3726.79 cm^{-1} on the SAC6:1 spectrum (Lou, et al., 2012; Shuit and Tan, 2014). The carbonyl C=O group from –COOH was attributed to wavenumbers 1653.79 to 1734.61 cm-1 in the AC600 spectrum and 1653.81 to 1752.34 cm-1 in the SAC6:1 spectrum as according to Dawodu, et al. (2014) and Konwar, et al (2014).

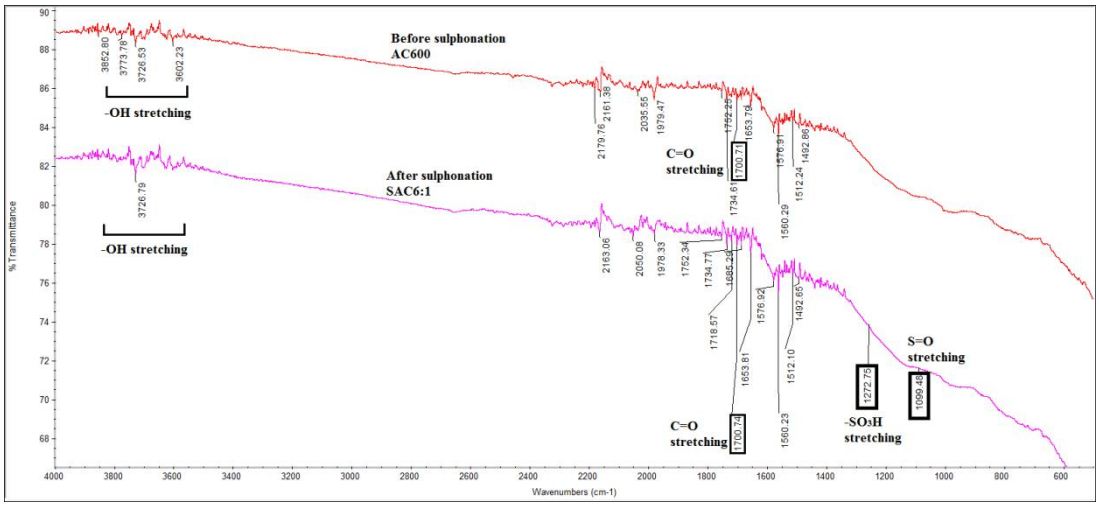

Figure 4.5: FT-IR Spectrum Before and After Sulphonation. The wavenumbers 1099.48 cm^{-1} and 1272.75 cm^{-1} corresponded to S=O and SO_3H stretching respectively, and their presence indicated the successful attachment of the SO_3H groups.

As mentioned in De, et al. (2015), functionalisation via 4-BDS has the advantage of preserving the structural and morphological properties of the carbon structure. Comparing both the SEM images of AC600 and SAC6:1 in Figure 4.6, it can be seen that sulphonation with 4-BDS did not alter the surface structure much as there was only a slight disintegration of the pores. This could be due to the action of the added phosphoric acid in activating the AC600 structure, slightly breaking down the carbon structure to allow the easier attachment of the SO_3H groups. Furthermore, the pore size before and after sulphonation remained almost the same at 1.5 µm. This justified the preservation of the catalyst morphology via 4-BDS sulphonation. Another added justification can be seen in the FT-IR spectra in Figure 4.5. A comparison of both spectra revealed infinitesimal changes to the spectra (besides the addition of the SO_3H group), solidifying the finding that 4-BDS sulphonation only exerted minute changes to the catalyst structure (Lou, et al., 2012).

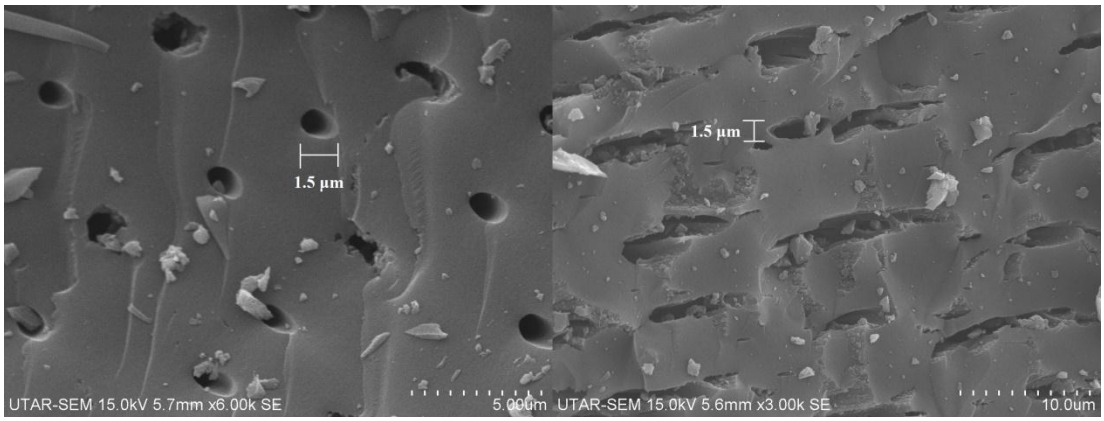

Figure 4.6: SEM Images Before (Left, AC600) and After Sulphonation (Right, SAC6:1)

Thermogravimetric analysis was performed on catalyst SAC6:1 and its thermal stability was compared to that of AC600. The results were plotted into Figure 4.7. The initial 7 % decrease in weight percentage from an initial temperature of 30 °C to 100 °C was due to the evaporation and loss of free water (Konwar, et al., 2014). The minute decrease in weight loss from 100 °C to 500 °C could be attributed to the removal of adsorbed water within the pores (Ezebor, et al., 2014; Zhou, et al., 2016). A more significant decrease was observed from 500 °C to 900 °C whereby the weight loss of the catalyst decreased by 20 % for SAC6:1 whereas the weight loss of AC600 was twice that value. This could be synonymous to removal of the SO_3H group as this region was absent in AC600 (Konwar, et al., 2014). This indicated that the sulphonated AC has a higher thermal stability compared to the unsulphonated AC. This was because the attachment of the SO_3H group lowered the inception of thermal decomposition (Konwar, et al., 2015). Therefore, it can be inferred from the Figure 4.7 that SAC6:1 has a thermal stability of up to 500 °C.

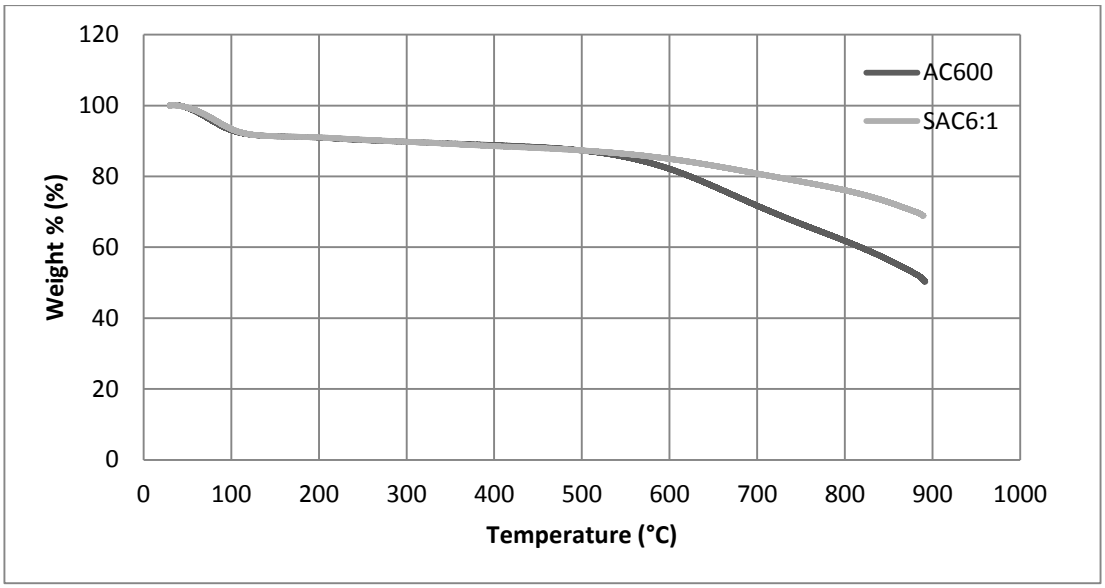

Figure 4.7: TGA Curve for AC600 and SAC6:1

X-Ray Diffraction patterns for both AC600 and SAC6:1 were shown in Figure 4.8. Looking at the diagram as a whole, it once more cemented the finding that sulphonation via 4-BDS maintained the structure of the support as no obvious differences could be seen between the two XRD profiles. According to both Ezebor, et al. (2014) and Zhou, et al. (2016), the diffraction peaks observed at $2\theta = 20\ ° – 35\ °$ corresponded to aromatic carbon sheets arranged randomly in an amorphous structure, with a plane of (002) (Konwar et al., 2014). The peaks at $2\theta = 40\ ° – 55\ °$ could be credited to its crystalline graphite-like structure (Zhou et al., 2016), which according to Konwar, et al (2014), had a plane of (101). The two sharp peaks located at $2\theta = 65\ °$ and $2\theta = 78\ °$ could be ascribed to impurities introduced during blending (aluminium from the blender blade) or carbonisation (silica from the crucible).

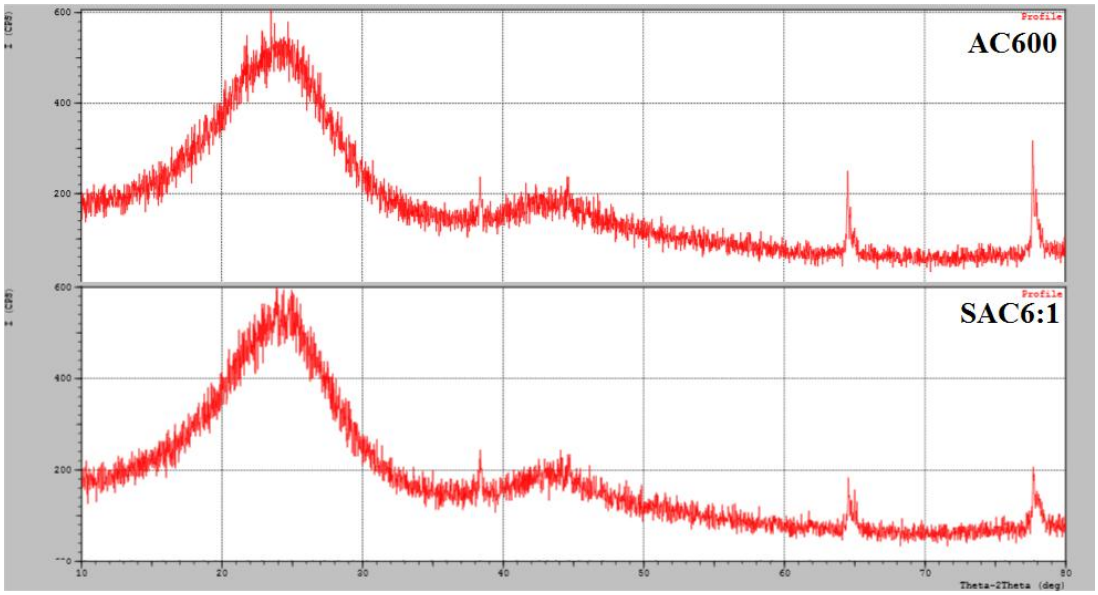

Figure 4.8: XRD Profile of AC600 (Top) and SAC6:1 (Bottom)

A comparison of numerous novel carbon catalysts and the catalyst produced in this study was done and generated in Table 4.4. It should be noted that all the catalyst listed were synthesised via sulphonation with 4-BDS.

Table 4.4: Comparison of SAC6:1 and Other Carbon Catalysts From Various Literatures

Carbon source	**BET surface area (m^2/g)**	**Total acid density (mmol/g)**	**Source**
Rubber seed shell	238	2.89	
Activated carbon power	318	1.42	Geng, et al. (2011)
Carbon-coated alumina (CCA)	39	1.72	
CCA with alumina removed	354	1.49	
Oil-cake waste	556	0.735	Konwar, et al. (2014)
***J.curcas* De-oiled seed waste cake (DOWC)**	93	3.96	Konwar, et al. (2015)
***P. pinnata* De-oiled seed waste cake (DOWC)**	483	3.62	

Comparing the rubber seed shell-derived SAC to novel carbon catalyst synthesised by others, it could be seen that SAC6:1 has a higher total acid density value than that of the catalyst developed by Geng, et al. (2011) and Konwar, et al. (2014). This indicated that rubber seed shells could be a good candidate in synthesising a promising solid acid catalyst to be used in biodiesel production. It is therefore hypothesised that a high FFA conversion would come out of this experimentation.

4.3 Biodiesel Characterisation

Esterification of palm fatty acid distillate (PFAD) was carried out at 90 °C with a catalyst loading of 3 wt%, and by varying the methanol-to-oil ratio (from 5:1 to 25:1) and duration (3 h to 8 h) to investigate the conversion of the free fatty acids (FFA) within PFAD into biodiesel. FFA conversion was calculated based on the acid values by using Eq. (4.1):

$$Conversion\ (\%) = \frac{AV - AV_0}{AV_0} \tag{4.1}$$

Where AV and AV_0 were the final and initial acid values respectively. The acid value was found according to the methodology in Sub-subsection 3.5.1 and is calculated using Eq. (4.2) as shown:

$$AV(mg\ KOH^{-1}) = \frac{56.1 \times M \times V}{W} \tag{4.2}$$

Where

M = molarity of the solution, M

V = volume of KOH reacted, cm^3

W = the weight of the sample, g

The effect of methanol-to-oil ratio on the FFA conversion of PFAD was illustrated in Figure 4.6.

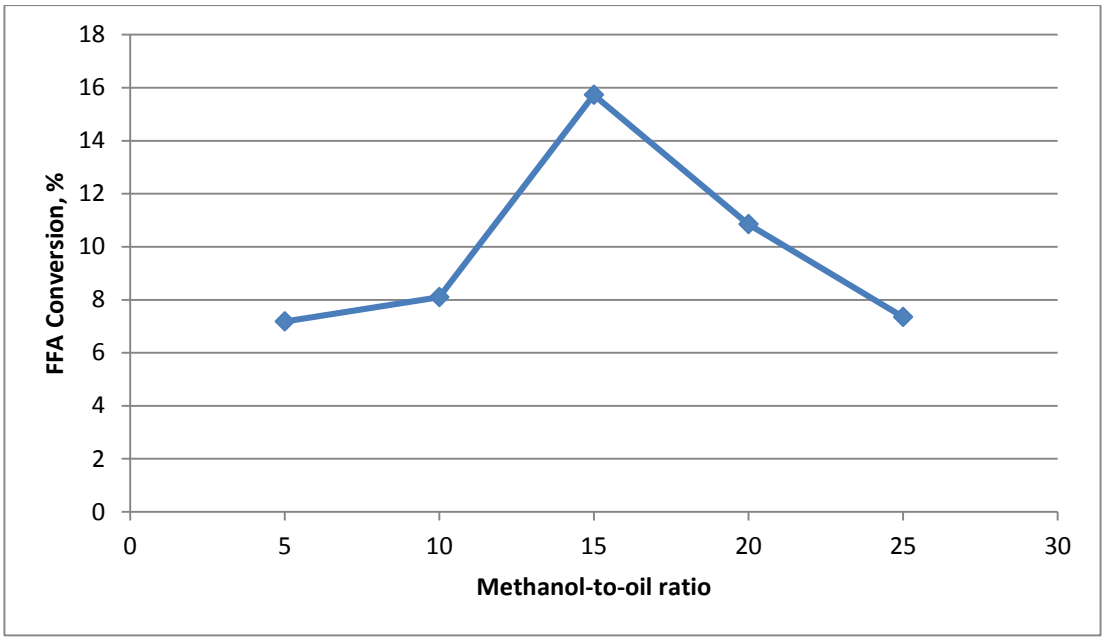

Figure 4.9: Effect of Methanol-to-Oil Ratio on FFA Conversion. The reaction temperature was 90 °C, with a catalyst loading of 3 wt% and a duration of 2.5 h.

It can be seen in Figure 4.9 that as the amount of methanol increased, the FFA conversion improved greatly until it reached a peak conversion of about 16% at a ratio of 15:1. After this peak, it showed a linear decline until it reached a minimum FFA conversion of about 7%. Hence, the optimum methanol-to-oil ratio was determined to be 15:1 in this experiment.

As the esterification reaction was a reversible reaction, increasing the concentration of methanol would inadvertently increase the fatty acid methyl esters (FAME) production as the equilibrium shifted forward according to Le Chatelier's Principle. Therefore, it was always preferable to have methanol in excess of a 1:1 stoichiometric ratio (Ezebor, et al., 2014). According to Zhou, et al. (2016), increasing methanol concentration was beneficial as this improved the hydrophilicity of the catalyst and the miscibility of methanol and the free fatty acids. Despite this, excessive methanol would dilute the reaction system, reducing the frequency of collision or even shield the FFA molecules from the active sites on the catalyst.

Jiang, et al. (2013) further justified that too much methanol would cause it to adsorb and accumulate on the catalyst surface, deactivating the catalyst and offsetting the increase in FFA conversion. In other words, as the methanol-to-oil ratio increased, the catalyst concentration in the system decreased as more catalysts were deactivated, which caused a decrease in conversion.

The effect of esterification duration on the FFA conversion of PFAD was illustrated in Figure 4.10.

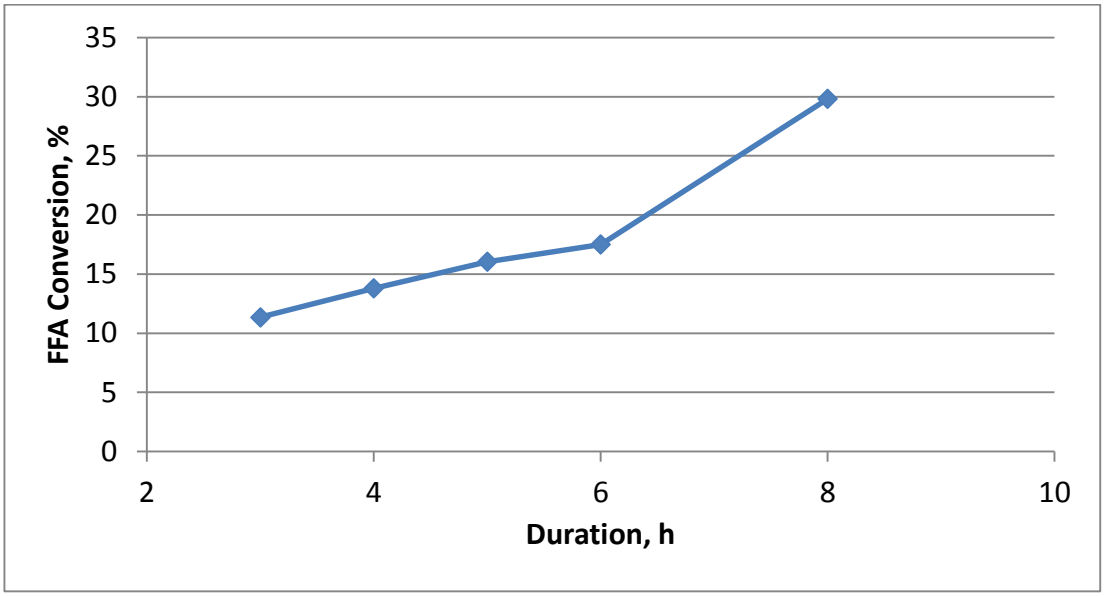

Figure 4.10: Effect of Esterification Duration on FFA Conversion. The reaction temperature was 90 °C, with a catalyst loading of 3 wt% and a methanol-to-oil ratio of 15:1.

Figure 4.10 shows that for every one hour increase in reaction time from 3 h to 6 h, the FFA conversion gradually increased from a conversion of around 11 % to a value of around 17 %. A further increase in esterification duration up to 8 h increased the FFA conversion further to about 30 %.

In the beginning of the reaction, the methanol and PFAD molecules start to collide with the SAC. The attachment of both the PFAD and methanol molecules led to the formation of methyl esters and water. As the reaction time increased, the frequency of collision between the reactant molecules and the catalyst increased, leading to an increase in methyl ester formation. As the catalysts were not involved in the reaction and its conformation was not changed, the methanol and PFAD molecules could weakly bind to the active sites for esterification to take place before detaching and allowing other reactants to take their places. This reaction would carry on indefinitely until all the reactants have been converted into FAME. Therefore, the graph still continued to increase after a duration of 8 h as the reactants have not been used up. It is thus determined that the optimum esterification duration for this experiment was 8 h.

Once again, esterification reaction is a reversible reaction which not only produces methyl esters in the forward reaction but water too. Thence, there could be setbacks in prolonging the reaction as this could inadvertently increase the water content within the mixture, driving the esterification reaction backwards. But judging on the trend in Figure 4.10, the FFA conversion has not reached a plateau after 8 h. This could mean that the reactants were still dominating within the mixture compared to the products, so the reaction was still being driven forward as according to Le Chatelier's Principle.

Compared to the conversion values obtained in Geng, et al. (2012), Konwar, et al. (2014), and Malins, et al. (2015), the conversion values obtained in this experiment was comparatively lower than all three journals. The types of carbon precursor used, its acid density, the esterification conditions, maximum duration and final conversion of each literature were summarised in Table 4.5. By comparing the acid densities of each catalyst, the SAC derived from rubber seed shells should give the highest FFA conversion as compared to the other catalysts. The fact that the results showed otherwise could mean that there might be more weak acid sites present on the surface of the catalyst as compared to the number of strong acid sites.

Table 4.5: Comparison of Esterification Duration and Conversion of Various Literatures

Carbon Precursor	**Acid Density and Esterification Conditions**	**Longest Duration (h)**	**Conversion (%)**	**Source**
Rubber seed shells	Acid density = 2.89 mmol/g T = 90 °C Loading = 3 wt% Methanol:oil ratio = 15:1	8	30	-
Resin	Acid density = 1.86 mmol/g T = 65 °C Loading = 20 mg of solid catalyst Methanol = 8 ml Oleic acid = 1 g	5	97	Geng, et al (2012)
Oil-cake waste	Acid density = 2.426 mmol/g T = 100 °C Loading = 5 wt% Methanol to oil ratio = 43:1	6	97	Konwar, et al. (2014)
Activated carbon	Acid density = 0.72 mmol/g T = 65 °C Loading = 10 wt% Methanol to oil ratio = 20:1	7	92	Malins, et al. (2015)

The low conversion could also be attributed to the low catalyst loading as compared to Konwar, et al (2014) and Malins, et al. (2015). This was because at low catalyst loading, there were fewer SACs available to bring both the methanol molecules and the PFAD molecules in close contact with each other to react. Moreover, faulty equipment could have contributed to the low FFA conversion. When carrying out the experiment, the temperature probe of the heating mantle was not in contact with the solution mixture, instead was placed on the surface of the round bottom flask near the bottom. Therefore, the temperature reading on the heating mantle did not represent the actual temperature of the solution mixture, and

the actual temperature within the round bottom flask could be lower. Hence, the conversion was at a low value.

In addition, if it were true that there were a higher number of weaker –OH acid groups located on the catalyst as compared to the strong SO_3H acid groups, sulphonation via 4-BDS could not be a plausible method when using rubber seed shells as a carbon precursor. Stronger sulphonating agent, such as concentrate or fuming sulphuric acid, could be a more effective candidate due to its more rigorous nature, although there is always the setback of it affecting the structural morphology of the catalyst. Besides, non-conventional sulphonating agents mentioned in Subsection 2.3.1, which were *p*-toluenesulphonic acid (PTSA), in-situ polymerisation of acetic anhydride, in-situ polymerisation of poly(sodium 4-styrenesulphonate) and thermal decomposition of ammonium sulphate could also be tested to decide on the best sulphonating agent when using rubber seed shells as the carbon precursor.

CHAPTER 5

CONCLUSIONS AND RECOMMENDATIONS

5.1 Conclusions

In conclusion, the objective to synthesise a heterogeneous carbon-based solid acid catalyst using waste rubber seed shells via the 4-Benzenediazoniumsulphonate (4-BDS) method was successfully achieved. Both the carbonisation temperature and sulphanilic acid-to-activated carbon ratio for the synthesis of the carbon-based solid acid catalyst were successfully optimised. The catalytic activity of the novel catalyst for biodiesel production was investigated and the esterification conditions (methanol-to-oil ratio and esterification duration) were successfully optimised.

The study showed that as carbonisation temperature increased, the specific surface area of the carbonised material increased. The optimal carbonsation temperature within the range of study was found to be 600 °C. High sulphanilic acid-to-activated carbon ratios improve the total acid density of the sulphonated material. The optimal ratio was found to be 6:1 for the catalyst produced. Based on the results from the Sorptomatic Surface Area Analyser, the specific surface area of the catalyst was 238 m^2/g. The pore diameter of the catalyst according to the SEM images was found to be 1.5 μm. The FT-IR spectrum not only showed the successful attachment of the SO3H groups at 1099.48 cm^{-1} and 1272.75 cm^{-1}, but EDX and total acid density tests showed that the catalyst has an elemental sulphur composition of 7.22 wt% and a total acid density of 2.894 $mmol/g_{cat}$. TGA analysis indicated that the SAC6:1 catalyst has a thermal stability of up to 500 °C. XRD patterns showed that the catalyst produced was an amorphous aromatic carbon structure with a plane of (002) and a plane of (101).

The catalytic activity of the catalyst was found to be dependent on methanol-to-oil ratios and esterification duration. At 90 °C with a catalyst loading of 3 wt%, the optimal methanol-to-oil ratio was found to be 15:1 whereas the optimal duration was 8 h. The free fatty acid (FFA) conversion of palm fatty acid distillate (PFAD) under optimal conditions was found to be 30 %. Rubber seed shells have the potential to be used as a carbon precursor in SAC synthesis for biodiesel production.

5.2 Recommendations for future work

It would be recommended that the same weighing balance be used as the calibration between devices could have minor changes. Extended laboratory hours could aid in obtaining better and more reliable results for time-dependent reactions. A larger container should be used in preparing the ice bath in order for low temperatures to be maintained throughout the experiment. When drying, samples should be left longer within the dryer to ensure moisture is completely removed. It can also be recommended that a proper functioning heating mantle should be used to ensure the readings obtained from the heating mantle.

REFERENCES

Ayodele, O.O. and Dawodu, F.A., 2014. Production of biodiesel from Calophyllum inophyllum oil using a cellulose-derived catalyst. *Biomass and Bioenergy*, 70, pp.239-48.

Berkeleybiodiesel.org, 2015. *Usage of Biodiesel Fuel - A Review by Experts*. [Online] Available at: http://www.berkeleybiodiesel.org/usage-of-biodiesel-fuel-a.html [Accessed 3 February 2017].

Bloomberg News, 2012. *Condoms, gloves provide lifeline for Malaysian rubber*. [Online] Available at: http://www.bangkokpost.com/print/322063/ [Accessed 3 March 2017].

Borhan, A. and Kamil, A.F., 2012. Preparation and Characterization of Activated Carbon from Rubber-seed Shell by Chemical Activation. *Journal of Applied Sciences*, 12(11), pp.1124-29.

Campbell, C.J., 2005. Future Production - Crisis and Beyond. In *Oil Crisis*. Borough of Brentwood: Multi-Science Publishing Co. Ltd. pp.173-76.

Chen, G. and Fang, B.S., 2011. Preparation of solid acid catalyst from glucose–starch mixture for biodiesel production. *Bioresource Technology*, 102(3), pp.2635–40.

Choi, J.M., Han, S.S. and Kim, H.S., 2015. Industrial Applications for Enzyme Biocatalysis: Current Status and Future Aspects. *Biotechnology Advances*, 33(7), pp.1443-54.

CIEC Promoting Science, 2013. *Catalysis in Industry*. [Online] Available at: http://www.essentialchemicalindustry.org/processes/catalysis-in-industry.html [Accessed 25 January 2017].

Clark, J., 2013. *Le Chatelier's Principle*. [Online] Available at: http://www.chemguide.co.uk/physical/equilibria/lechatelier.html [Accessed 9 February 2017].

Dawodu, F.A. et al., 2014. Effective conversion of non-edible oil with high free fatty acid into biodiesel by sulphonated carbon catalyst. *Applied Energy*, 114, pp.819–26.

De, S., Balu, A.M., van der Waal, J.C. and Luque, R., 2015. Biomass-Derived Porous Carbon Materials: Synthesis and Catalytic Applications. *ChemCatChem*, 7, pp.1608 – 1629.

Demshimino, S.I. et al., 2013. Comparative Analysis of Biodiesel and Petroleum Diesel. *International Journal of Education and Research*, 1(8), pp.1-8.

Diesel Service and Supply, 2017. *Industrial Diesel Engines: Generator and Engine Types and Industrial Uses*. [Online] Available at:

http://www.dieselserviceandsupply.com/industrial_industry_usage.aspx [Accessed 21 January 2017].

Ezebor, F., Khairuddean, M., Abdullah, A.Z. and Boey, P.L., 2014. Oil palm trunk and sugarcane bagasse derived heterogeneous acid catalysts for production of fatty acid methyl esters. *Energy*, 70, pp.493–503.

Fu, X.B. et al., 2015. Biodiesel Production Using a Carbon Solid Acid Catalyst Derived from β-Cyclodextrin. *Journal of the American Oil Chemists' Society*, 92(4), pp.495-502.

Fu, X.B. et al., 2013. A microalgae residue based carbon solid acid catalyst for biodiesel production. *A microalgae residue based carbon solid acid catalyst for biodiesel*, 146, pp.767–70.

Gardy, J., Hassanpour, A., Lai, X.J. and Ahmed, M.H., 2016. Synthesis of Ti(SO4)O solid acid nano-catalyst and its application for biodiesel production from used cooking oil. *Applied Catalysis A: General*, 527, pp.81-95.

Geng, L., Wang, Y., Yu, G. and Zhu, Y.X., 2011. Efficient carbon-based solid acid catalysts for the esterification of oleic acid. *Catalysis Communications*, 13(1), pp.26-30.

Geng, L., Yu, G., Wang, Y. and Zhu, Y.X., 2012. Ph-SO3H-modified mesoporous carbon as an efficient catalyst for the esterification of oleic acid. *Applied Catalyst A: General*, 427-428, pp.137-44.

Guldhe, A. et al., 2017. Biodiesel synthesis from microalgal lipids using tungstated zirconia as a heterogeneous acid catalyst and its comparison with homogeneous acid and enzyme catalysts. *Fuel*, 187, pp.180-88.

Guo, F., Xiu, Z.L. and Liang, Z.X., 2012. Synthesis of biodiesel from acidified soybean soapstock using a lignin-derived carbonaceous catalyst. *Applied Energy*, 98, pp.47–52.

Haluzan, D., 2010. Biodiesel and Standard Diesel Comparison. *Renewables-info.com*, 23 November.

Hara, M., 2010. Biodiesel Production by Amorphous Carbon Bearing SO3H, COOH and Phenolic OH Groups, a Solid Brønsted Acid Catalyst. *Topics in Catalysis*, 53(11), pp.805-10.

Hays, J., 2008. *Rubber in Malaysia*. [Online] Available at: http://factsanddetails.com/southeast-asia/Malaysia/sub5_4e/entry-3702.html#chapter-1 [Accessed 3 March 2017].

Hexza Corporation Berhad, 2016. *Subsidiaries Profile*. [Online] Available at: http://www.hexza.com.my/sub_hexzachem_sarawak.htm [Accessed 13 February 2017].

HORIBA, 2017. *SA-9600 BET Surface Area Analyzer*. [Online] Available at: http://www.horiba.com/scientific/products/particle-characterization/surface-area-analysis/details/sa-9600-series-938/ [Accessed 25 February 2017].

Jiang, Y.W. et al., 2013. Esterification of oleic acid with ethanol catalyzed by sulfonated cation exchange resin: Experimental and kinetic studies. *Energy Conversion and Management*, 76, pp.980-85.

Konwar, L.J., Boro, J. and Deka, D., 2014. Review on latest developments in biodiesel production using carbon-based catalysts. *Renewable and Sustainable Energy Reviews*, 29, pp.546–64.

Konwar, L.J. et al., 2014. Biodiesel production from acid oils using sulfonated carbon catalystderived from oil-cake waste. *Journal of Molecular Catalysis A: Chemical*, 388-389, pp.167–76.

Konwar, L.J. et al., 2015. Towards carbon efficient biorefining: Multifunctional mesoporous solid acids obtained from biodiesel production wastes for biomass comversion. *Applied Catalysis B: Environmental*, 176-177, pp.20-35.

Kotrba, R., 2016. *Finland's Chinese-owned synthetic diesel plant*. [Online] Available at: http://biodieselmagazine.com/blog/article/2016/02/finlands-chinese-owned-synthetic-diesel-plant [Accessed 3 February 2017].

Lal, R., 2005. World Crop Residues Production and Implications of Its Use as a Biofuel. *Environmental International*, 31(4), pp.575-84.

Liu, T.T. et al., 2013. Preparation and characterization of biomass carbon-based solid acid catalyst for the esterification of oleic acid with methanol. *Bioresource Technology*, 133, pp.618–21.

Lokman, I.M., Rashid, U. and Taufiq-Yap, Y.H., 2015. Production of biodiesel from palm fatty acid distillate using sulfonated-glucose solid acid catalyst: Characterization and optimization. *Chinese Journal of Chemical Engineering*, 23(11), pp.1857–64.

Lou, W.Y. et al., 2012. A Highly Active Bagasse-Derived Solid Acid Catalyst with Properties Suitable for Production of Biodiesel. *ChemSusChem*, 5(8), pp.1-10.

Lou, W.Y., Zong, M.H. and Duan, Z.Q., 2008. Efficient production of biodiesel from high free fatty acid-containing waste oils using various carbohydrate-derived solid acid catalysts. *Bioresource Technology*, 99(18), pp.8752–58.

Malins, K. et al., 2015. Synthesis of activated carbon based heterogenous acid catalyst for biodiesel preparation. *Applied Catalysis B*, 176-177, pp.553-58.

Martinot, E., 2008. *Organisations Engaged in Renewable Energy*. [Online] Available at: http://www.martinot.info/organizations.htm [Accessed 3 February 2017].

Materials Evaluation and Engineering, Inc., 2017. *FOURIER TRANSFORM INFRARED SPECTROSCOPY (FTIR)*. [Online] Available at: http://www.mee-inc.com/hamm/fourier-transform-infrared-spectroscopy-ftir/ [Accessed 25 February 2017].

Merchant Research & Consulting, Ltd, 2017. *Biodiesel: 2017 World Market Outlook and Forecast up to 2021*. [Online] Available at: https://mcgroup.co.uk/researches/biodiesel [Accessed 4 February 2017].

Mo, X.H. et al., 2008. Activation and deactivation characteristics of sulfonated carbon catalysts. *Journal of Catalysis* , 254, pp.332-38.

Pagketanang, T., Artnaseaw, A., Wongwicha, P. and Thabuot, M., 2015. Microporous Activated Carbon from KOH-Activation of Rubber Seed-Shells for Application in Capacitor Electrode. *Energy Procedia*, 79, pp.651-56.

Perkin Elmer, 2015. *Thermogravimetric Analysis (TGA)*. Waltham: Perkin Elmer, Inc.

REN21, 2016. *Renewables 2016: Global Status Report*. Paris: REN21 REN21.

Ross, M.L., 2013. How the 1973 Oil Embargo Saved the Planet. *Foreign Affairs*, 15 October.

Rubber Board, 2002. *Experimentally Proved Uses of Rubber Seed Oil*. [Online] Available at: http://rubberboard.org.in/ManageCultivation.asp?Id=229 [Accessed 3 March 2017].

Shimadzu Corporation, 2017. *Gas Chromatography*. [Online] Available at: http://www.shimadzu.com/an/gc/index.html [Accessed 25 February 2017].

Shu, Q. et al., 2010. Synthesis of biodiesel from waste vegetable oil with large amounts of free fatty acids using a carbon-based solid acid catalyst. *Applied Energy*, 87(8), pp.2589-96.

Shuit, S.H. and Tan, S.H., 2014. Feasibility study of various sulphonation methods for transforming carbon nanotubes into catalysts for the esterification of palm fatty acid distillate. *Energy Conversion and Management*, 88, pp.1283-89.

Shu, Q. et al., 2009. Synthesis of biodiesel from cottonseed oil and methanol using a carbon-based solid acid catalyst. *Fuel Processing Technology*, 90(7-8), pp.1002–08.

Swapp, S., 2017. *Scanning Electron Microscopy (SEM)*. [Online] Available at: http://serc.carleton.edu/research_education/geochemsheets/techniques/SEM.html [Accessed 25 February 2017].

Talha, N.S. and Sulaiman, S., 2016. Overview of Catalysts in Biodiesel Production. *Journal of Engineering and Applied Sciences*, 11(1), pp.439-48.

Thermo ARL, 1999. *Basics of X-Ray Diffraction*. [Online] ThermoARL Available at: https://old.vscht.cz/clab/RTG/dokumenty/thermo/xrd/Introduction%20to%20powder%20diffraction.pdf [Accessed 20 August 2017].

TutorVista.com, 2017. *Homogeneous Catalyst - Definition, Mechanism & Example*. [Online] Available at: http://chemistry.tutorvista.com/inorganic-chemistry/homogeneous-catalyst.html [Accessed 4 February 2017].

U.S. Department of Energy, 2017. *Biodiesel Blends*. [Online] Available at: http://www.afdc.energy.gov/fuels/biodiesel_blends.html [Accessed 4 February 2017].

U.S. Energy Information Administration, 2016. *Use of Diesel - Energy Explained, Your Guide to Understanding Energy*. [Online] Available at: http://www.eia.gov/Energyexplained/index.cfm?page=diesel_use [Accessed 21 January 2017].

U.S. Energy Information Administration, 2017. *Biofuels: Ethanol and Biodiesel - Energy Explained, Your Guide to Understanding Energy*. [Online] Available at: http://www.eia.gov/energyexplained/index.cfm/data/index.cfm?page=biofuel_home [Accessed 4 February 2017].

U.S. Energy Information Administration, 2017. *Short-Term Energy Outlook*. [Online] Available at: https://www.eia.gov/outlooks/steo/report/global_oil.cfm [Accessed 23 January 2017].

University of California, 2016. *Electron Dispersive X-Ray Spectroscopy*. [Online] Available at: http://cfamm.ucr.edu/documents/eds-intro.pdf [Accessed 25 February 2017].

USDA Foreign Agricultural Service, 2016. *Brazil: Annual Report 2016*. Washington: USDA USDA.

USDA Foreign Agricultural Service, 2016. *EU-28: Annual Report 2016*. Washington: USDA USDA.

USDA Foreign Agricultural Service, 2016. *Indonesia: Annual Report 2016*. Washington: USDA USDA.

USDA Foreign Agricultural Service, 2016. *Malaysia: Annual Report 2016*. Washington: USDA USDA.

Williams, M., 2016. *What Percent of Earth is Water?* [Online] Available at: http://www.universetoday.com/65588/what-percent-of-earth-is-water/ [Accessed 3 February 2017].

Yang, Y.X., Chiang, K. and Burke, N., 2011. Porous carbon-supported catalysts for energy and environmental applications: A short review. *Catalysis Today*, 178(1), pp.197–205.

Zhou, Y., Niu, S.L. and Li, J., 2016. Activity of the carbon-based heterogeneous acid catalyst derived from bamboo in esterification of oleic acid with ethanol. *Energy Conversion and Management*, 114, pp.188-96.

Zillillah, Toh, A.N. and Zhi, L., 2014. Phosphotungstic Acid-Functionalised Magnetic Nanoparticles as an Efficient and Recyclable Catalyst for the One-Pot Production of Biodiesel from Grease via Esterification and Transesterification. *Green Chemistry*, 16(3), pp.1202-10.

Zong, M.H. et al., 2007. Preparation of a sugar catalyst and its use for highly efficient production of biodiesel. *Green Chemistry*, 9(5), pp.434-37.

APPENDICES

APPENDIX A: Gantt Chart

No	Project Activities	W1	W2	W3	W4	W5	W6	W7	W8	W9	W10	W11	W12	W13	W14
M1	Gathering of materials and glassware														
M2	Biomass carbonisation														
M3	AC sulphonation														
M4	Catalyst characterisation														
M5	Esterification of PFAD														
M6	Biodiesel characterisation														
M7	Report writing & Presentation														

APPENDIX B: BET Sorptomatic Surface Analyser Results

APPENDIX C: X-Ray Diffraction Results